

Federated PCA on Grassmann Manifold for IoT Anomaly Detection

Tung-Anh Nguyen, Long Tan Le, Tuan Dung Nguyen,
 Wei Bao, *Member, IEEE*, Suranga Seneviratne, *Senior Member, IEEE*,
 Choong Seon Hong, *Fellow, IEEE*, Nguyen H. Tran, *Senior Member, IEEE*.

Abstract—With the proliferation of the Internet of Things (IoT) and the rising interconnectedness of devices, network security faces significant challenges, especially from anomalous activities. While traditional machine learning-based intrusion detection systems (ML-IDS) effectively employ supervised learning methods, they possess limitations such as the requirement for labeled data and challenges with high dimensionality. Recent unsupervised ML-IDS approaches such as AutoEncoders and Generative Adversarial Networks (GAN) offer alternative solutions but pose challenges in deployment onto resource-constrained IoT devices and in interpretability. To address these concerns, this paper proposes a novel federated unsupervised anomaly detection framework – FedPCA – that leverages Principal Component Analysis (PCA) and the Alternating Directions Method Multipliers (ADMM) to learn common representations of distributed non-i.i.d. datasets. Building on the FedPCA framework, we propose two algorithms, FEDPE in Euclidean space and FEDPG on Grassmann manifolds. Our approach enables real-time threat detection and mitigation at the device level, enhancing network resilience while ensuring privacy. Moreover, the proposed algorithms are accompanied by theoretical convergence rates even under a sub-sampling scheme, a novel result. Experimental results on the UNSW-NB15 and TON-IoT datasets show that our proposed methods offer performance in anomaly detection comparable to non-linear baselines, while providing significant improvements in communication and memory efficiency, underscoring their potential for securing IoT networks.

Index Terms—Federated Learning, Internet of Things, Consensus Optimization, Grassmann Manifolds, Anomaly Detection.

I. INTRODUCTION

THE ubiquity of Internet of Things (IoT) technologies has led to a transformative shift where intelligent devices exchange information and enact decisions via the internet, requiring minimal human intervention. This has significantly enhanced the quality of life and found applications across numerous sectors such as smart city infrastructures [1], energy systems [2], or climate systems [3]. However, as the IoT ecosystem expands and becomes increasingly complex, ensuring robust network security emerges as a paramount task, especially considering the inherent security vulnerabilities of many IoT devices due to their limited computational resources [4].

T.-A. Nguyen, L. T. Le, N. H. Tran, W. Bao, and S. Seneviratne are with the School of Computer Science, The University of Sydney, Sydney, NSW 2006, Australia (email: tung6100@uni.sydney.edu.au, {long.le, nguyen.tran, wei.bao, suranga.seneviratne}@sydney.edu.au). T. D. Nguyen is currently with the Department of Computer and Information Science, University of Pennsylvania, USA (email: joshtn@seas.upenn.edu). C. S. Hong is with the Department of Computer Science and Engineering, School of Computing, Kyung Hee University, Yongin-si 17104, Republic of Korea (email: cshong@khu.ac.kr).

In this intricate landscape, machine learning-based intrusion detection systems (ML-IDS) form a crucial line of defense. These systems often utilize supervised learning methods that range from traditional techniques to more sophisticated deep learning approaches [5]. While effective in various scenarios, they come with several limitations. For instance, they necessitate access to a considerable volume of *labeled data*, which can be time-consuming and costly to generate. Additionally, they often struggle with *high-dimensional data* and are limited in their ability to detect novel anomalies not represented in the training data. In contrast, recent unsupervised ML-IDS methods, such as AutoEncoders [6] and GAN-based models [7], [8], provide anomaly detection by learning representation of normal behavior without relying on labeled data. However, these techniques often involve training deep neural network models, which can be computationally demanding and lack clear interpretability [9] – factors that pose significant challenges for resource-limited IoT devices.

Traditionally, most ML-IDS lean on centralized deployment which is becoming less feasible in IoT networks due to privacy concerns and resource limitations. Hence, there's a heightened demand for distributed security frameworks where IoT devices can have self-monitoring capabilities that allow them to identify potential threats in their network traffic while contributing their insights to the broader system. Such a distributed approach would considerably enhance the resilience of IoT networks, enabling real-time anomaly detection and mitigation in heterogeneous environments. In light of this, Federated Learning (FL) has stepped in as a promising paradigm that allows IoT devices to collaboratively learn a shared model while retaining their data locally, thereby harmonizing privacy preservation and efficient resource utilization. *Despite its potential, the exploration of federated unsupervised IDS under the heterogeneity of IoT traffic remains relatively nascent*, indicating the need for further research in this area.

In response to these challenges, we introduce a novel federated unsupervised anomaly detection framework that leverages the representation power of PCA [10] and the decomposability of ADMM [11], namely FedPCA [12]. Specifically, we aim to harness PCA's capabilities to learn a common representation of distributed non-i.i.d datasets via consensus optimization that captures the hidden states within the data. These hidden states typically reflect complex correlations and underlying patterns within the data, which are instrumental in effective anomaly detection. In order to solve FedPCA, we design two distinct algorithms including FedPCA in Euclidean space (FEDPE) and

FedPCA on Grassmann manifolds (FEDPG). Each algorithm possesses unique properties offering potential advantages for FL. While FEDPE operates within a Euclidean space affording both simplicity and interpretability, FEDPG projects the data onto Grassmann manifolds providing an efficient way to handle the high-dimensional, complex, and potentially exhibit non-linear structures of network data. We then investigate their convergence characteristics and provide convergence guarantees under standard assumptions. Our proposed FL framework offers notable advantages: it preserves privacy while providing efficient anomaly detection in resource-constrained environments.

Within this work, each IoT device functions as an anomaly detection system, playing an active role in fortifying the system's security. The devices continuously monitor their communication patterns, employing anomaly detection models to identify abnormal behaviors that could signify a potential threat. By deploying ML-IDS at the IoT device level, we establish a distributed network of vigilant sentinels, each capable of real-time threat identification. It enables IoT devices to partake in the learning process without sharing sensitive local data—a characteristic of paramount importance in an IoT setting where user data privacy is highly valued. This setup substantially enhances the resilience and security of the entire IoT network, and requires a shorter detection time compared to its unsupervised counterparts. The main contributions of this work can be summarized as follows:

- We propose an unsupervised federated PCA framework for efficient host-based IoT anomaly detection, which is formulated by a consensus optimization problem for privacy-preserving and communication-efficient.
- We introduce a new algorithm designed for FEDPE and FEDPG based on ADMM-based procedures with client sub-sampling schemes aiming to enhance robustness and mitigate communication bottlenecks.
- We provide the theoretical convergence analysis for the proposed framework, showing that it converges to a stationary point where the consensus constraint is satisfied.
- Through experiments on the UNSW-NB15 [13] and TON-IoT network [14] datasets, we demonstrate that FEDPE and FEDPG not only show competitive performance against non-linear methods in anomaly detection but also boast significant improvements in communication and memory efficiency. The extensive evaluation showcases the robustness of our proposed framework to non-i.i.d. data distribution, marking it well-suited for IoT networks.

The rest of the paper is organized as follows. Section II outlines the relevant background and previous works that closely relate to our topics of interest. The problem formulation and the proposed framework are introduced in Section III with a detailed explanation of algorithm designs. In Section IV, we present theoretical convergence analyses for the proposed algorithms. Numerical results and conclusion are conducted in Section V and Section VI, respectively.

II. RELATED WORKS

A. Federated Learning

Federated Learning (FL) represents a cutting-edge distributed learning approach that allows for the execution and subsequent updating of machine learning models across thousands of participating devices, while simultaneously safeguarding against data leaks [15]. In FL, models are deployed and trained locally on individual clients' devices using local data. These locally trained models are then transmitted back to the central server for aggregation, such as weight averaging [16]. Thanks to the attributes of efficient communication and privacy protection, FL proves highly advantageous for IoT networks and applications. Various versions of FL have been developed after the birth of the standard FedAvg [16], significantly augmenting the intelligence of IoT systems across a multitude of applications [17].

The primary challenges of FL can be broadly classified into two categories: *communication bottlenecks*, resulting from the need to exchange large model's parameters between parties, and *data heterogeneity*, arising from the diversity of the data held by FL clients. This motivated some prior works to design more communication-efficient strategies such as local updates [18]–[20], model compression [21], and adaptive communication [22]. Meanwhile, data heterogeneity concerned with clients' non-i.i.d. data has also been well-studied [23], [24].

B. Optimization on Grassmann Manifolds

Grassmann manifold optimization has recently gained traction as an advanced mathematical tool in the fields of machine learning. This approach leverages the geometric properties of Grassmann manifolds, a space representing linear subspaces, to facilitate the analysis and understanding of high-dimensional data, thereby enabling efficient optimization and enhanced modeling in various machine learning and data analysis tasks [25]. In centralized learning, the optimization over Grassmann manifolds has been employed to enhance manifold learning and data classification, with applications extending to computer vision and speech recognition [26]–[28]. In decentralized learning contexts, particularly in FL, Grassmann learning has not fully explored yet, making it a promising avenue for continued research and development.

C. IoT Anomaly Detection

Owing to their inherent vulnerabilities, IoT systems require robust measures against malicious activities [29]. This need has propelled anomaly-based Intrusion Detection Systems (IDS) into the limelight, bolstered by the radical advancements in machine learning. Early research on anomaly-based IDS within IoT networks has been heavily centered around methodologies where data is consolidated onto a central server [30]–[35], raising concerns related to privacy and cyber intrusions.

The recent trend has veered towards the use of FL frameworks for network anomaly detection. For example, Nguyen et al. [36] developed a federated intrusion detection system using Recurrent Neural Network models that were trained on local gateways and then amalgamated into a single model. Similarly, Wang et al. [37] demonstrated how a feed-forward artificial neural network can augment detection performance. Mothukuri

et al. [38] employed federated training on Gated Recurrent Units (GRUs) models, preserving data on local IoT devices by only sharing the learned weights with the central server. However, accurately detecting unknown anomalous activities has proven challenging, given the inherent imbalance between normal and abnormal traffic in IoT networks [4].

D. Principal Component Analysis

Over recent years, PCA [39] has become a popular unsupervised learning model in centralized machine learning. From an IoT security standpoint, PCA-based anomaly detection has emerged as an efficient technique, with PCA deployed to bifurcate a dataset into benign and malicious subspaces [40]. For instance, Brauckhoff et al. [41] suggested the use of the Karhunen-Loeve expansion in light of the data's temporal correlation, albeit limited to data from a single router. Kernel PCA has been put forward to examine features considering both variance and mean [42]. However, these methods, while promising, are constrained by their reliance on data from a single device, rendering them inadequate for IDS in settings where resources are limited and privacy is paramount.

Distributed PCA has gained traction in the machine learning community [43]. For example, Ge et al. [44] proposed a min-max optimization framework for generating a distributed sparse PCA estimator while maintaining privacy. Grammenos et al. [45] suggested an asynchronous FL method to implement PCA in a memory-limited environment, introducing an algorithm that calculates local model updates using a streaming process and adaptively estimates its principal components.

E. ADMM-based Learning

The Alternating Direction Method of Multipliers (ADMM) has made significant advancements in both theory and application over recent decades [11]. ADMM acts as a powerful framework that combines the strengths of dual decomposition and the method of multipliers to solve optimization problems. The core idea behind this framework is to break down a problem into simpler subproblems that can be solved in parallel, and then combine the solutions of these subproblems to arrive at a global solution. The mathematical and convergence characteristics of ADMM have been well-studied in the literature [46]–[49].

Owing to its decompositional nature, ADMM has found significant applications in large-scale and distributed optimization tasks, especially in machine learning [50], [51]. In FL, several ADMM-based decentralized methods have been developed to enhance communication efficiency [52], [53]. However, employing this framework for distributed PCA is still uncharted.

In this study, we employ an alternative strategy to develop an effective unsupervised method for network anomaly detection in IoT systems. We propose an unsupervised federated PCA framework grounded in ADMM-based learning, addressing privacy concerns while efficiently detecting anomalies in both recognized and unprecedented attacks.

III. PROBLEM FORMULATION

A. Federated Principal Component Analysis

We consider an IoT network comprised of a central global coordinator CO and a set of N IoT devices, each denoted

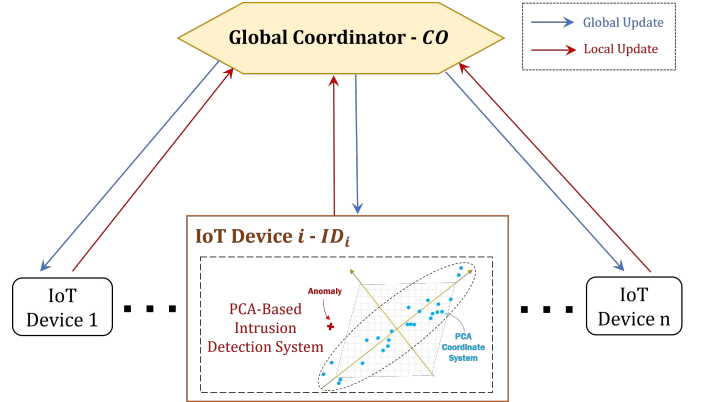


Fig. 1: Overview of a host-based IoT anomaly detection system utilizing Federated PCA.

by a unique identifier ID_i holding a local data set X_i , where $i \in 1, 2, \dots, N$. This network interacts within a client-server topology, as depicted in Fig. 1. Our framework employs a host-based IDS strategy, where each IoT device operates as a sentinel within the network, examining its network traffic and identifying potential security threats. This distributed approach significantly increases the network's resilience by facilitating real-time threat detection and mitigation. Furthermore, since the learning is local to each device, it allows for a reduction in communication overhead and strengthens privacy by keeping the data on the device.

Principal Component Analysis Revisiting: We first revisit the basics of PCA to formally define our method. PCA projects a given dataset X onto principal components ordered by the amount of variance they capture in the data [54]. Specifically, it seeks an optimal rank- k ($k < d$) matrix \tilde{X} that minimizes the reconstruction error $\|X - \tilde{X}\|_F$, where $\|\cdot\|_F$ denotes the Frobenius norm [55]. Typically, \tilde{X} is derived based on the singular value decomposition (SVD) of X , i.e., $X = U\Sigma V^\top$, where $U \in \mathbb{R}^{d \times d}$ is an orthonormal matrix containing the left singular vectors of X , $\Sigma = \text{diag}(\sigma_1, \dots, \sigma_d)$ contains the singular values ($\sigma_1 \geq \sigma_2 \geq \dots \geq \sigma_d$), and $V \in \mathbb{R}^{D \times D}$ contains the right singular vectors of X . Let $U^{(k)} \in \mathbb{R}^{d \times k}$ be the first k columns of U and $\Sigma_k = \text{diag}(\sigma_1, \dots, \sigma_k)$. We can rewrite the solution for \tilde{X} as

$$\tilde{X} = U^{(k)} U^{(k)\top} X, \quad (1)$$

which can be interpreted as the projection of data matrix X onto the column space of $U^{(k)}$. The PCA problem can thus be formulated as an optimization problem as follows:

$$\begin{aligned} \min_{U \in \mathbb{R}^{d \times k}} \quad & \| (I - U U^\top) X \|_F^2 \\ \text{s.t.} \quad & U^\top U = I. \end{aligned} \quad (2)$$

The essence of this problem is to locate an orthogonal matrix U that minimizes the reconstruction error of X when projected onto the column space of U , resulting in a matrix $Z = U^\top X \in \mathbb{R}^{k \times D}$ provides a lower-dimensional representation of X .

In the context of developing ML-IDS for IoT networks, solving this PCA problem typically requires IoT devices to transmit their local data to a centralized server. While this approach offers a streamlined method for anomaly detection, it is

hampered by two main obstacles. First, data transferring within the resource-limited and bandwidth-constrained landscape of IoT can lead to significant *communication bottlenecks*, which in turn might escalate operational costs, amplify latency, and induce network congestion. Second, the act of centralizing such data amplifies *privacy concerns* as it risks exposing sensitive information from personal environments, posing serious threats to user confidentiality. Hence, an alternative would be to seek distributed methods that address these issues while still effectively detecting anomalies.

Federated PCA via ADMM Consensus Optimization:

To address these concerns, we propose a federated approach for solving PCA on distributed datasets, namely FedPCA, which aims to collectively learn a *common representation* from all local datasets, X_1, X_2, \dots, X_N , without the *CO* directly accessing these datasets. We first introduce a set of local variables U_1, \dots, U_N , where U_i is the local PCA matrix learned by client i . Then, we formulate a consensus optimization problem as follows:

$$\begin{aligned} \min_{U_1, \dots, U_N} \quad & \sum_{i=1}^N \|(I - U_i U_i^\top) X_i\|_F^2 \\ \text{s.t.} \quad & U_i = Z, \quad \forall i = 1, \dots, N, \\ & U_i^\top U_i = I, \quad \forall i = 1, \dots, N, \end{aligned} \quad (3)$$

where the first linear constraint enforces the “consensus” to a *common low-rank matrix* Z [56] for all local U_i . The second constraint ensures that the matrix U_i is orthonormal for every client keeping the distributed problem consistent with the classical centralized PCA. However, addressing the non-linearity introduced by this orthonormality constraint is a challenging task due to the non-convex nature of the problem. Here, we employ a surrogate technique, as introduced in [46], to handle the above non-linear constraint as follows.

$$h_i(U_i) = \max \{0, U_i^\top U_i - I\}^2, \quad (4)$$

where the operators max and squared are component-wise. By reformulating the problem to the $h_i(U_i)$ function, we gently steer the optimization towards matrices U_i that approach orthonormality, making the landscape more tractable for iterative frameworks. We then have the problem (3) equivalent to the following:

$$\begin{aligned} \min_{U_1, \dots, U_N} \quad & \sum_{i=1}^N \|(I - U_i U_i^\top) X_i\|_F^2 \\ \text{s.t.} \quad & U_i = Z, \quad \forall i = 1, \dots, N \\ & h_i(U_i) \leq 0, \quad \forall i = 1, \dots, N. \end{aligned} \quad (5)$$

Given the nature of problem (5) as a consensus optimization with linear constraints, we opt to utilize ADMM [11] for its resolution. The essence of this iterative framework is the alternating updates of primal and dual variables to achieve two main objectives: the U_i across clients converge towards a common Z and the objective function is iteratively minimized. Applying this to our problem, we first construct the augmented Lagrangian function associated with the problem (5) as follows.

Algorithm 1 FedPCA in Euclidean Space (FEDPE)

```

1: Randomly initialize  $Z^0$  and  $U_i^0$ ,  $\forall i = 1, \dots, N$ 
2: for  $k = 0, \dots, T - 1$  do
3:   Sample subset clients  $\mathcal{S}^k$ 
4:   for each client  $i \in \mathcal{S}^k$  in parallel do
5:      $U_i^{k+1} = \arg \min_{U_i} \left\{ f_i(U_i) + \langle Y_i^k, U_i - Z^k \rangle_F + \langle T_i^k, h_i(U_i) \rangle_F + \frac{\rho}{2} \|U_i - Z^k\|_F^2 + \frac{\rho}{2} \|h_i(U_i)\|_F^2 \right\}$ 
6:   end for
7:    $CO$  updates  $Z^{k+1} = \frac{1}{|\mathcal{S}^k|} \sum_{i \in \mathcal{S}^k} (U_i^{k+1} + \frac{1}{\rho} Y_i^k)$ 
8:    $CO$  broadcasts  $Z^{k+1}$  to all clients
9:   for each client  $i \in \mathcal{S}^k$  in parallel do
10:     $Y_i^{k+1} = Y_i^k + \rho (U_i^{k+1} - Z^{k+1})$ 
11:     $T_i^{k+1} = T_i^k + \rho h_i(U_i^{k+1})$ 
12:   end for
13: end for

```

$$\begin{aligned} \mathcal{L}(\{U_i\}, Z, \{Y_i\}, \{T_i\}) = & \sum_{i=1}^N f_i(U_i) + \sum_{i=1}^N \langle Y_i, U_i - Z \rangle_F \\ & + \sum_{i=1}^N \langle T_i, h_i(U_i) \rangle_F + \frac{\rho}{2} \sum_{i=1}^N \|U_i - Z\|_F^2 + \frac{\rho}{2} \sum_{i=1}^N \|h_i(U_i)\|_F^2, \end{aligned} \quad (6)$$

where $f_i(U_i) = \|(I - U_i U_i^\top) X_i\|_F^2$ is the objective function, $\langle \cdot, \cdot \rangle_F$ is the Frobenius inner product between two matrices.

This augmented Lagrangian makes the optimization problem more amenable to iterative solution techniques while ensuring that constraints are respected. The terms with Lagrange multipliers (or dual variables) – $\sum_{i=1}^N \langle Y_i, U_i - Z \rangle_F$ and $\sum_{i=1}^N \langle T_i, h_i(U_i) \rangle_F$ – quantify the influence of the constraints on achieving a common PCA representation across distributed datasets. They ensure that each local PCA matrix U_i converges to a shared matrix Z and adheres to the non-linear constraints dictated by $h_i(U_i)$. On the other hand, the penalty terms – $(\rho/2) \sum_{i=1}^N \|U_i - Z\|_F^2$ and $(\rho/2) \sum_{i=1}^N \|h_i(U_i)\|_F^2$ – are governed by the penalty parameter ρ to penalize any deviation of the local PCA matrices U_i from the global consensus matrix Z or from satisfying the orthogonality conditions $h_i(U_i)$.

Since, the Frobenius inner product for matrices is analogous to the standard dot products for vectors, we can obtain the gradients of the augmented Lagrangian (6) w.r.t. dual variables Y_i and T_i as follows.

$$\nabla_{Y_i} \mathcal{L}_\rho(U, Z, Y, T) = U_i - Z$$

$$\nabla_{T_i} \mathcal{L}_\rho(U, Z, Y, T) = h_i(U_i)$$

To solve the proposed problem, we employ an ADMM-based procedure in which a subset of clients, denoted as \mathcal{S}^k , performs iterative updates using a step size ρ during the k -th communication round as follows.

1) Primal Update (Local Update):

$$\begin{aligned} U_i^{k+1} = \arg \min_{U_i} & \left\{ f_i(U_i) + \langle Y_i^k, U_i - Z^k \rangle_F + \langle T_i^k, h_i(U_i) \rangle_F \right. \\ & \left. + \frac{\rho}{2} \|U_i - Z^k\|_F^2 + \frac{\rho}{2} \|h_i(U_i)\|_F^2 \right\} \end{aligned} \quad (7)$$

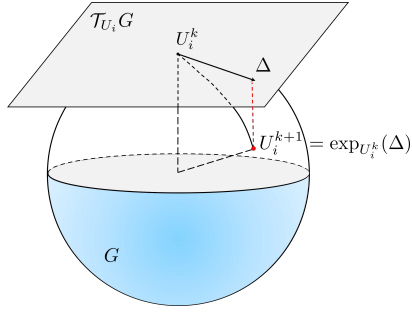


Fig. 2: Illustration of movement on a Grassmann manifold, represented by a sphere. Given a point U_i^k on Grassmann manifold G and a vector Δ on the tangent space denoted by $\mathcal{T}_{U_i}G$ at U_i^k , a point U_i^{k+1} is identified by exponential mapping $\exp_{U_i^k}(\Delta)$. In our context, the manifold G contains all matrix U_i satisfy the condition $U_i^\top U_i = I$.

2) *Consensus Update (Global Update):*

$$Z^{k+1} = \frac{1}{|\mathcal{S}_k|} \sum_{i \in \mathcal{S}_k} \left(U_i^{k+1} + \frac{1}{\rho} Y_i^k \right) \quad (8)$$

3) *Dual Update (Local Updates):*

$$Y_i^{k+1} = Y_i^k + \rho (U_i^{k+1} - Z^{k+1}) \quad (9)$$

$$T_i^{k+1} = T_i^k + \rho h_i(U_i^{k+1}). \quad (10)$$

When $|\mathcal{S}_k| = N$, substituting Z^{k+1} to Y_i^{k+1} results in $\frac{1}{N} \sum_{i=1}^N Y_i^{k+1} = 0$. This which means Z update can be rewritten as [56]:

$$Z^{k+1} = \frac{1}{N} \sum_{i=1}^N U_i^{k+1}. \quad (11)$$

These steps are repeated iteratively until convergence, at which point the local PCA matrix U_i and the consensus variable Z agree, resulting in a common matrix learned from the distributed data. This ADMM-based framework collaboratively drives towards a consensus PCA solution while ensuring that the unique characteristics of each dataset are preserved.

The above procedure is denoted as FedPCA in Euclidean space, abbreviated as FEDPE. The full procedure is detailed in Alg. 1. Specially, in each round, a distinct subset of clients \mathcal{S}_k is selected to perform the update (Alg. 1, line 3). Each selected client is then involved in solving the primal problem (7) on Euclidean space locally using gradient-based methods (Alg. 1, line 5). Once finishing training, selected clients send their local PCA matrix to the *CO* for updating the common PCA matrix Z (Alg. 1, line 7). Finally, each selected client i update its dual variable Y_i and T_i based on the latest U_i and Z (Alg. 1, lines 10-11). One main difference between FEDPE in this work and the one presented in [12] is that we employ a client subsampling strategy during the federated training process. This offers significant benefits, including reduced communication overhead, improved scalability for large-scale IoT networks, and enhanced resilience to stragglers or non-responsive devices.

B. FedPCA using ADMM on Grassmann Manifold

Although FEDPE effectively addresses the proposed problem, we further extend its capacity by formulating FedPCA

on Grassmann manifolds, denoted as FEDPG, to accelerate convergence. Notably, the orthonormality constraint utilized in (3) signifies that the parameters of (7) can be projected onto a Grassmann manifolds [25].

Orthonormality meets the Grassmannian: The Grassmann manifold, denoted as $G(n, d)$, represents a geometric space that encapsulates sets of d -dimensional subspaces within an overaching n -dimensional real or complex Euclidean space, subject to $n \geq d > 0$ [25]. The distinct of this manifold lies in its representation capacity: Any point on $G(n, d)$ can be identified by an $n \times d$ orthogonal matrix U whose column spans the corresponding subspace to ensure orthonormality $U^\top U = I_d$. Hence, $G(n, d)$ is defined as follows.

$$G(n, d) = \{\text{span}(U) : U \in \mathbb{R}^{n \times d}, U^\top U = I_d\} \quad (12)$$

Fig. 2 shows an example of the Grassmann manifold as the surface of a sphere. Here, the tangent space $\mathcal{T}_U G$ at U captures the set of all directions in which the subspace can "move" but still stay very close to the manifold. By capturing the space of all orthonormal subspaces, the Grassmann manifold offers an elegant framework for addressing optimization problems with orthonormality constraints (e.g., problem (3)) since these constraints are automatically maintained when operations are performed within this manifold.

FedPCA via Grassmann Manifold Optimization: By framing problem (3) within the Grassmann manifold, the augmented Lagrangian (6) evolves as follows.

$$\begin{aligned} \mathcal{L}(\{U_i\}, Z, \{Y_i\}) \\ = \sum_{i=1}^N f_i(U_i) + \sum_{i=1}^N Y_i^\top (U_i - Z) + \frac{\rho}{2} \sum_{i=1}^N \|U_i - Z\|_F^2. \end{aligned} \quad (13)$$

Here, the terms associated with $h_i(U_i)$ are eliminated because the inherent orthonormality constraints are satisfied.

Denoting the local update for each client i at the k -th iteration by following:

$$F_i^k(U_i) := f_i(U_i) + Y_i^{k\top} (U_i - Z^k) + \frac{\rho}{2} \|U_i - Z^k\|_F^2 \quad (14)$$

We then recast the update rules for U_i and Z on the Grassmann manifold as follows.

$$U_i^{k+1} = \arg \min_{U_i} \left\{ F_i^k(U_i) \right\} \quad (15)$$

As detailed in Alg. 2 (lines 5-8), projected gradient descent on the Grassmann manifold is applied in every local iteration in clients to find the update of U_i^{k+1} in (15). Considering the definition of the Grassmann manifold in (12), we enforce the second constraint $U_i^\top U_i = I$ by using the projected gradient descent on the Grassmann manifold (Alg. 2, line 8) as follows

$$U_i^{k+1} = R(U_i^k - \eta \nabla_U F_i^k(U_i^k)), \quad (16)$$

Here, η is the step size and $\nabla_U F_i^k(U_i^k)$ is the gradient of $F_i^k(U_i^k)$ at the point U_i^k , and the retraction function $R(\cdot)$ is the projection operation performed by QR decomposition [25]. The projection process for U_i^k and U_i^{k+1} is graphically illustrated in Fig. 2. We compute the updates by projecting the Euclidean gradient onto the tangent space of the manifold using orthogonal projection $F_i^k(U_i^k) \rightarrow \nabla_U F_i^k(U_i^k)$ (Alg. 2,

Algorithm 2 FedPCA on Grassmann Manifold (FEDPG)

```

1: Randomly initialize  $Z^0$  and  $U_i^0$ ,  $\forall i = 1, \dots, N$ 
2: for  $k = 1, \dots, T$  do
3:   Sample subset clients  $\mathcal{S}^k$ 
4:   for each client  $i \in \mathcal{S}^k$  in parallel do
5:      $U_i^{k,0} = U_i^k$ 
6:     for  $c = 1, \dots, C$  do
7:        $\nabla_U F_i^k(U_i^{k,c}) = (I_d - U_i^{k,c} U_i^{k,c\top}) F_i^k(U_i^{k,c})$ 
8:        $U_i^{k,c+1} = R(U_i^{k,c} - \eta \nabla_U F_i^k(U_i^{k,c}))$ 
9:     end for
10:     $U_i^{k+1} = U_i^{k,C}$ 
11:   end for
12:    $CO$  updates  $Z^{k+1} = \frac{1}{|\mathcal{S}^k|} \sum_{i \in \mathcal{S}^k} (U_i^{k+1} + \frac{1}{\rho} Y_i^k)$ 
13:    $CO$  broadcasts  $Z^{k+1}$  to all clients
14:   for each client  $i \in \mathcal{S}^k$  in parallel do
15:      $Y_i^{k+1} = Y_i^k + \rho (U_i^{k+1} - Z^{k+1})$ 
16:   end for
17: end for

```

line 7) as follows.

$$\nabla_U F_i^k(U_i^k) = (I_d - U_i^k U_i^{k\top}) F_i^k(U_i^k). \quad (17)$$

Note that Equations (16) and (17) are repeatedly updated in C local rounds to solve Equation (15) (Alg. 2, lines 6-9).

The use of Grassmannian gradients in FEDPG enables more precise and effective steps toward the optimal solution, thus accelerating convergence. Furthermore, PCA problems often include orthogonality constraints, which are complex to handle in traditional Euclidean spaces and slow the convergence rate. FEDPG elegantly deals with these constraints by projecting the problem onto the Grassmann manifold, where orthogonality constraints are naturally satisfied. By doing so, it eliminates the need for extra steps to manage these constraints, reducing computational overhead and facilitating faster convergence.

Moreover, FEDPG ensures an exact solution due to its unique feature of projection onto the Grassmann manifold. This process maintains the inherent orthogonality conditions that PCA requires, effectively preserving the constraints of the original problem. Therefore, the solutions derived from FEDPG are precise and exact as they are always in the feasible region. On the other hand, FEDPE's solutions are approximations. While FEDPE works effectively in solving the problem, it doesn't inherently uphold the orthogonality conditions. The resulting solutions, therefore, might be outside the feasible region, and additional steps are necessary to bring the solution back into the feasible space. This could lead to approximation errors, and therefore the solutions are not always exact.

IV. FEDPCA: CONVERGENCE ANALYSIS

In this section, we present a theoretical analysis to understand the convergence properties of FEDPG and FEDPE within the FedPCA framework. To begin with, we consider an FL environment with N clients, indexed by $i = 1, 2, \dots, N$, and introduce the following notations for the analyses:

- 1) $\mathcal{S}^k \subset \{1, 2, \dots, N\}$: denotes the subset of clients selected in the k -th iteration.

- 2) $k(i)$: denotes the latest iteration at which the client i has its model updated.

The orthonormality constraint in (3) is a critical component for our proposed method. While FEDPE handles this by introducing a surrogate linear constraint in (4), FEDPG relaxes this by leveraging projected gradient descent on Grassmann manifolds. Hence, to ensure the generality of our framework, we employ the augmented Lagrangian (13) and rewrite it to adapt for the convergence analysis of both algorithms as follows.

$$\begin{aligned} \mathcal{L}(\{U_i\}, Z, \{Y_i\}) = & \sum_{i=1}^N f_i(U_i) + \sum_{i=1}^N Y_i^\top (U_i - Z) \\ & + \frac{\rho_i}{2} \sum_{i=1}^N \|U_i - Z\|_F^2 \end{aligned} \quad (18)$$

s.t. $U_i^\top U_i = I$.

In addition, we modify the global update (8) by following:

$$Z^{k+1} = \frac{1}{|\mathcal{S}_k|} \sum_{i \in \mathcal{S}_k} (U_i^{k+1} + \frac{1}{\rho_i} Y_i^k) \quad (19)$$

Accordingly, the local updates for U_i^{k+1} in (7) and Y_i^{k+1} in (9) at a selected client i will be changed as listed below.

$$\begin{aligned} U_i^{k+1} = \arg \min_{U_i} & \left\{ f_i(U_i) + \langle Y_i^k, U_i - Z^k \rangle_F \right. \\ & \left. + \frac{\rho_i}{2} \sum_{i=1}^N \|U_i - Z^k\|_F^2 \right\} \end{aligned} \quad (20)$$

$$\begin{aligned} \text{s.t. } & U_i^\top U_i = I \\ Y_i^{k+1} = & Y_i^k + \rho_i (U_i^{k+1} - Z^{k+1}) \end{aligned} \quad (21)$$

It is worth noting that this modification does not affect the performance of FEDPE and FEDPG since the update results will be the same after one iteration.

Assumption. We first make the following assumptions:

- A1: For each client's objective function $f_i, \forall i = 1, \dots, N$ there exists a constant $L_i \geq 0$ such that for any two points U_i, Z_i , the gradient of f_i satisfies the Lipschitz condition: $\|\nabla f_i(U_i) - \nabla f_i(Z_i)\|_F \leq L_i \|U_i - Z_i\|_F, \forall i$
- A2: For all i , the penalty parameter ρ_i is chosen large enough such that the U_i sub-problem (20) is strongly convex with modulus $\mu_i(\rho_i)$.
- A3: $\mathcal{L}(x)$ is bounded from below, i.e.,

$$\underline{\mathcal{L}} := \min_X \mathcal{L}(X) > -\infty$$

Remark IV.1. Assumptions A1 and A3 are standard in analyzing convergence properties for ADMM. Under Assumption A2, as ρ_i increases, the subproblem (20) will be eventually strongly convex with respect to U_i . The associated strong convexity modulus $\mu_i(\rho_i)$ is a monotonic increasing function of ρ_i .

To establish a convergence guarantee of FEDPE and FEDPG, we aim to show the following. Start with the variables $(\{U_i^k\}, Z^k, \{Y_i^k\})$. After T rounds (i.e., after all clients have participated at least once since iteration k), the new variables $(\{U_i^{k+T}\}, Z^{k+T}, \{Y_i^{k+T}\})$ lead to decrease in the global

augmented Lagrangian \mathcal{L} . Then we show these variables will converge to a local stationary point of \mathcal{L} . Notably, our analysis employs matrix variables, in contrast to other ADMM-based methods using vector variables [46]–[49]

A. Bound on the Successive Difference of Dual Variables

We establish an upper bound for the successive difference of the dual variables Y_i in terms of the primal variables U_i .

Lemma IV.2. *Suppose Assumptions A1 hold, then we have*

$$\|Y_i^{k+1} - Y_i^k\|_F^2 \leq L_i^2 \|U_i^{k+1} - U_i^k\|_F^2, \forall i, \forall k \quad (22)$$

Proof. In the case of $i \notin S^k$, (22) is true because both sides of (22) are equal to zero. When $i \in S^k$, we have below equation from optimal condition for (20).

$$\nabla f_i(U_i^{k+1}) + Y_i^k + \rho_i(U_i^{k+1} - Z^{k+1}) = 0 \quad (23)$$

Substituting (23) to the dual variable update (21), the following equation is derived.

$$\nabla f_i(U_i^{k+1}) = -Y_i^{k+1} \quad (24)$$

Combining with Assumption A1, and noting that for any given i , U_i and Y_i are updated in the same iteration, we obtain for all $i \in S^k \setminus \{0\}$:

$$\begin{aligned} \|Y_i^{k+1} - Y_i^k\|_F &= \|\nabla f_i(U_i^{k+1}) - \nabla f_i(U_i^{k(i)})\|_F \\ &= \|\nabla f_i(U_i^{k+1}) - \nabla f_i(U_i^{k(i)})\|_F \\ &\leq L_i \|U_i^{k+1} - U_i^{k(i)}\|_F = L_i \|U_i^{k+1} - U_i^k\|_F \end{aligned}$$

B. Bound for the Augmented Lagrangian

Next, we show that the augmented Lagrangian (18) can be decreased sufficiently and bounded below.

Lemma IV.3. *Suppose Assumption A1, A2 and A3 hold, then the augmented Lagrangian is bounded as follows.*

$$\begin{aligned} &\mathcal{L}(\{U_i^{k+1}\}, Z^{k+1}, \{Y_i^{k+1}\}) - \mathcal{L}(\{U_i^k\}, Z^k, \{Y_i^k\}) \\ &\leq \sum_{i \in S^k} \left(\frac{L_i^2}{\rho_i} - \frac{\mu_i}{2} \right) \|U_i^{k+1} - U_i^k\|_F^2 - \frac{\gamma}{2} \|Z^{k+1} - Z^k\|_F^2 \end{aligned}$$

Proof. For each client $i \in S^k$, we can split the successive difference of the augmented Lagrangian by following.

$$\begin{aligned} &\mathcal{L}(\{U_i^{k+1}\}, Z^{k+1}, \{Y_i^{k+1}\}) - \mathcal{L}(\{U_i^k\}, Z^k, \{Y_i^k\}) \\ &= \underbrace{\mathcal{L}(\{U_i^{k+1}\}, Z^{k+1}, \{Y_i^{k+1}\}) - \mathcal{L}(\{U_i^{k+1}\}, Z^{k+1}, \{Y_i^k\})}_A \\ &\quad + \underbrace{\mathcal{L}(\{U_i^{k+1}\}, Z^{k+1}, \{Y_i^k\}) - \mathcal{L}(\{U_i^{k+1}\}, Z^k, \{Y_i^k\})}_B \\ &\quad + \underbrace{\mathcal{L}(\{U_i^{k+1}\}, Z^k, \{Y_i^k\}) - \mathcal{L}(\{U_i^k\}, Z^k, \{Y_i^k\})}_C \quad (25) \end{aligned}$$

Bounding Term A. The first term in (25) can be bounded as follows.

$$\begin{aligned} &\mathcal{L}(\{U_i^{k+1}\}, Z^{k+1}, \{Y_i^{k+1}\}) - \mathcal{L}(\{U_i^{k+1}\}, Z^{k+1}, \{Y_i^k\}) \\ &= \sum_{i=1}^N \langle Y_i^{k+1} - Y_i^k, U_i^{k+1} - Z^{k+1} \rangle_F \\ &\stackrel{(a)}{=} \sum_{i \in S^k} \frac{1}{\rho_i} \|Y_i^{k+1} - Y_i^k\|_F^2 \end{aligned} \quad (26)$$

where (a) is achieved by using (21).

Bounding Term B. The second term in (25) can be bounded as follows.

$$\begin{aligned} &\mathcal{L}(\{U_i^{k+1}\}, Z^{k+1}, Y^k) - \mathcal{L}(\{U_i^{k+1}\}, Z^k, \{Y_i^k\}) \\ &\stackrel{(A2)}{\leq} \sum_{i=1}^N \left(\langle \nabla_{U_i} \mathcal{L}(\{U_i^{k+1}\}, Z^{k+1}, Y^k), U_i^{k+1} - U_i^k \rangle \right. \\ &\quad \left. - \frac{\mu_i}{2} \|U_i^{k+1} - U_i^k\|_F^2 \right) \\ &\stackrel{(b)}{=} - \sum_{i \in S^+} \frac{\mu_i}{2} \|U_i^{k+1} - U_i^k\|_F^2. \end{aligned} \quad (27)$$

where (b) is trivially true in the case of $i \notin S^k$ as $U_i^{k+1} = U_i^k$. In the case of $i \in S^k$, the $\nabla_{U_i} \mathcal{L}(\{U_i^{k+1}\}, Z^{k+1}, \{Y_i^k\}) = 0$ because of optimal condition of (20).

Bounding Term C. The third term in (25) can be bounded as follows.

$$\begin{aligned} &\mathcal{L}(\{U_i^{k+1}\}, Z^k, \{Y_i^k\}) - \mathcal{L}(\{U_i^k\}, Z^k, \{Y_i^k\}) \\ &\stackrel{(c)}{\leq} \sum_{i=1}^N \left(\langle \nabla_Z \mathcal{L}(\{U_i^k\}, Z^{k+1}, \{Y_i^k\}), Z^{k+1} - Z^k \rangle \right. \\ &\quad \left. - \frac{\gamma}{2} \|Z^{k+1} - Z^k\|_F^2 \right) \\ &\stackrel{(d)}{=} - \sum_{i \in S^k} \frac{\gamma}{2} \|Z^{k+1} - Z^k\|_F^2. \end{aligned} \quad (28)$$

where in (c) we used the fact that $\mathcal{L}(\{U_i\}, Z, \{Y_i\})$ is strongly convex w.r.t. Z .

For (d), it is trivially true if $i \notin S^k$ as $U_i^{k+1} = U_i^k$. When $i \in S^k$, the $\nabla_Z \mathcal{L}(\{U_i^k\}, Z^{k+1}, \{Y_i^k\}) = 0$ because of the optimal condition of (20).

Sufficient decrease. Combining the inequalities (26), (27) and (28) together, we have

$$\begin{aligned} &A + B + C \\ &= \mathcal{L}(\{U_i^{k+1}\}, Z^{k+1}, \{Y_i^{k+1}\}) - \mathcal{L}(\{U_i^k\}, Z^k, \{Y_i^k\}) \\ &\leq \sum_{i \in S^k} -\frac{\gamma}{2} \|Z^{k+1} - Z^k\|_F^2 + \left(\frac{L_i^2}{\rho_i} - \frac{\mu_i}{2} \right) \|U_i^{k+1} - U_i^k\|_F^2 \end{aligned} \quad (29)$$

This implies that the value of the augmented Lagrangian will always decrease if the following condition is satisfied:

$$\rho_i \mu_i \geq 2L_i^2 \quad (30)$$

Lower bound for the augmented Lagrangian. We continue showing that $\mathcal{L}(\{U_i^k\}, Z^k, \{Y_i^k\})$ convergence, i.e., \mathcal{L} is bounded below.

$$\begin{aligned}
\mathcal{L}(\{U_i^{k+1}\}, Z^{k+1}, \{Y_i^{k+1}\}) \\
&= \sum_{i=1}^N \left(f_i(U_i^{k+1}) + \langle Y_i^{k+1}, U_i^{k+1} - Z^{k+1} \rangle \right. \\
&\quad \left. + \frac{\rho_i}{2} \|U_i^{k+1} - Z^{k+1}\|_F^2 \right) \\
&\stackrel{(e)}{=} \sum_{i=1}^N \left(f_i(U_i^{k+1}) + \langle \nabla f(U_i^{k+1}), Z^{k+1} - U_i^{k+1} \rangle \right. \\
&\quad \left. + \frac{\rho_i}{2} \|U_i^{k+1} - Z^{k+1}\|_F^2 \right) \\
&\stackrel{(f)}{\geq} \sum_{i=1}^N f_i(Z^{k+1}) = \underline{\mathcal{L}}(Z^{k+1})
\end{aligned}$$

where (e) can be explained as following:

(e.1) If $i \in S^k$, based on (24):

$$\langle Y_i^{k+1}, U_i^{k+1} - Z^{k+1} \rangle = \langle \nabla f(U_i^{k+1}), Z^{k+1} - U_i^{k+1} \rangle$$

(e.2) If $i \notin S^k$, $Y_i^{k+1} = Y_i^k = Y_i^{k(i)}$, $U_i^{k+1} = U_i^k = U^{k(i)}$

$$\begin{aligned}
&\langle Y_i^{k+1}, U_i^{k+1} - Z^{k+1} \rangle \\
&= \langle \nabla f(U_i^{k(i)}), Z^{k+1} - U_i^{k(i)} \rangle \\
&= \langle \nabla f(U_i^{k+1}), Z^{k+1} - U_i^{k+1} \rangle
\end{aligned}$$

From combining (e.1) and (e.2), we deduce that (e) holds true. Consequently, due to the Lipschitz continuity of the gradient of f_i , (f) is also true.

Remark IV.4. Lemma IV.3 shows that the augmented Lagrangian decreases by a sufficient amount after each iteration. In practice, however, the penalty parameter ρ is difficult to estimate. Hence, for our experiments, we fine-tune ρ from a predefined range of values to select the best one.

C. Convergence of the augmented Lagrangian

Here, we combine Lemma (IV.2) and (IV.3) to establish the following theorem.

Theorem IV.5. Suppose the following are true:

- After T iterations, all clients have participated in training at least once.
- The global loss function $\mathcal{L}(Z^k, \{U_i^k\}, \{Y_i^k\})$ is bounded below by a finite quantity $\underline{\mathcal{L}}$.
- The hyperparameter ρ_i for the augmented Lagrangian is chosen such that $\rho_i \mu_i \geq 2L_i^2$.

Then the augmented Lagrangian \mathcal{L} will monotonically decrease and is convergent to a quantity of at least $\underline{\mathcal{L}}$. Further, for all $i = 1, \dots, N$ we have $\lim_{k \rightarrow \infty} \|Z^{k+T} - U_i^{k+T}\| = 0$.

Proof. Theorem IV.5 implies that the augmented Lagrangian decreases by a non-negative amount after every T global iterations. Given the fact that every client will be updated at least once in the interval $[k, k+T]$, we conclude that the limit $\lim_{k \rightarrow \infty} \mathcal{L}(Z^{k+T}, \{U_i^{k+T}\}, \{Y_i^{k+T}\})$ exists and is at least $\underline{\mathcal{L}}$.

Now we prove the second statement. From (29) and the fact that \mathcal{L} converges, we conclude that as $k \rightarrow \infty$,

$$\|Z^{k+T} - Z^k\| \rightarrow 0, \quad \|U_i^{k+T} - U_i^k\| \rightarrow 0.$$

Combining this with Lemma IV.2, we have $\|Y_i^{k+1} - Y_i^k\| \rightarrow 0$. Based on the definition of Y_i^{t+1} , this implies that

$$\|U_i^{k+1} - Z^{k+1}\| \rightarrow 0$$

Remark IV.6. Theorem IV.5 establishes that the sequence of primal and dual variables updated after each T global iterations of Algorithm 1 and Algorithm 2 converges. We further have $\|U_i^{k+1} - Z^{k+1}\| \rightarrow 0$, i.e., the consensus constraint is satisfied.

D. Convergence to stationary point

In the below theorem we present another guarantee that the limit of the sequence $(Z^k, \{U_i^k\}, \{Y_i^k\})$ is the a stationary solution for Problem (5).

Theorem IV.7. Suppose the assumptions in Theorem IV.5 hold. Then the limit point $(Z^*, \{U_i^*\}, \{Y_i^*\})$ of the sequence $(Z^k, \{U_i^k\}, \{Y_i^k\})$ is a stationary solution to Problem (5). That is, for all i ,

$$\nabla f_i(Z^*) + Y_i^* = 0 \text{ and } Z^* = U_i^*.$$

Proof. See the proof to [49, Theorem 2.4]. Here we make some remarks. First, because FEDPE and FEDPG allow for client sampling, the proof relies on an assumption that all clients will participate after some fixed number of rounds (in particular, T rounds). Second, since local objectives are smooth (possibly non-convex), the primal variables U_i are updated using first-order methods like SGD or projected GD. Finally, the proof aims to show that after every T rounds, we obtain a sufficient decrease in the augmented Lagrangian; coupled with the fact that the augmented Lagrangian is bounded below, the sequence of variables converges to a stationary point of \mathcal{L} .

E. Convergence rate of the augmented Lagrangian

We first define gradient of the Augmented Lagrangian as:

$$\hat{\nabla} \mathcal{L}(\{U_i\}, Z, Y) := \begin{bmatrix} \nabla_{U_1} \mathcal{L}(\{U_i\}, Z, Y) \\ \nabla_{U_2} \mathcal{L}(\{U_i\}, Z, Y) \\ \vdots \\ \nabla_{U_N} \mathcal{L}(\{U_i\}, Z, Y) \end{bmatrix}$$

We aim to use the below quantity to establish the progress of the proposed methods:

$$\begin{aligned}
P(\{U_i^k\}, Z^k, Y_i^k) &:= \sum_{i=1}^N \|U_i^k - Z^k\|^2 \\
&\quad + \|\hat{\nabla} \mathcal{L}(\{U_i^k\}, Z^k, Y_i^k)\|^2
\end{aligned}$$

It can be verified that if $P(\{U_i^k\}, Z^k, Y_i^k) \rightarrow 0$, then a stationary solution is obtained, which U_i converges to Z and gradient for Augmented Lagrangian of each client i is equal to zero.

Theorem IV.8. Suppose that Assumptions A.1, A.2, A.3 and Theorem IV.5 are satisfied. Let $T(\epsilon)$ denote an iteration index in which the following inequality is achieved:

$$T(\epsilon) := \min(\{k | P(\{U_i^k\}, Z^k, Y_i^k) \leq \epsilon, k \geq 0\})$$

for some $\epsilon > 0$. Then there exists some constant $\beta > 0$ such that

$$T(\epsilon) \leq \frac{\beta(\mathcal{L}(\{U_i^1\}, Z^1, Y_i^1) - \underline{\mathcal{L}})}{\epsilon}$$

where $\underline{\mathcal{L}}$ is defined by Assumption A.3.

Proof. Based on the optimal condition of U_i (7):

$$\nabla f_i(U_i^{k+1}) + Y_i^k + \rho_i(U_i^{k+1} - Z^{k+1}) = 0 \quad (31)$$

By definition of \mathcal{L} , we can have:

$$\begin{aligned} & \|\nabla_{U_i} \mathcal{L}(\{U_i^k\}, Z^k, Y_i^k)\| = \|\nabla f_i(U_i^k) + Y_i^k + \rho_i(U_i^k - Z^k)\| \\ & \stackrel{(g)}{=} \|\nabla f_i(U_i^k) + Y_i^k + \rho_i(U_i^k - Z^k) \\ & - (\nabla f_i(U_i^{k+1}) + Y_i^k + \rho_i(U_i^{k+1} - Z^{k+1}))\| \\ & \leq \|\nabla f_i(U_i^k) - \nabla f_i(U_i^{k+1})\| + \rho_i\|U_i^{k+1} - U_i^k\| \\ & + \rho_i\|Z^{k+1} - Z^k\| \\ & \stackrel{(h)}{\leq} L_i\|U_i^{k+1} - U_i^k\| + \rho_i\|U_i^{k+1} - U_i^k\| + \rho_i\|Z^{k+1} - Z^k\| \\ & = (L_i + \rho_i)\|U_i^{k+1} - U_i^k\| + \rho_i\|Z^{k+1} - Z^k\| \end{aligned} \quad (32)$$

Where (g) is obtained by optimal condition of U_i in (31). To derive (h), the first term is bounded by assumption A.1 and the second term is bounded by Lemma IV.2. Based on (32), we have the following:

$$\begin{aligned} \|\hat{\nabla} \mathcal{L}(\{U_i^k\}, Z^k, Y_i^k)\| & \leq \sum_{i=1}^N (L_i + \rho_i)\|U_i^{k+1} - U_i^k\| \\ & + \sum_{i=1}^N \rho_i\|Z^{k+1} - Z^k\| \end{aligned} \quad (33)$$

By taking $\sigma_1 = \max\{\sum_{i=1}^N \rho_i, L_1 + \rho_1, \dots, L_N + \rho_N\}$, it is apparent that $\sigma_1 > 0$. We can have following:

$$\|\hat{\nabla} \mathcal{L}(\{U_i^k\}, Z^k, Y_i^k)\| \leq \sigma_1(\|Z^{k+1} - Z^k\| + \sum_{i=1}^N \|U_i^{k+1} - U_i^k\|) \quad (34)$$

From (9), we have

$$\begin{aligned} \sum_{i=1}^N \|U_i^{k+1} - Z^{k+1}\| & = \sum_{i=1}^N \frac{1}{\rho_i} \|Y_i^{k+1} - Y_i^k\| \\ & \leq \sum_{i=1}^N \frac{L_i}{\rho_i} \|U_i^{k+1} - U_i^k\| \end{aligned} \quad (35)$$

(34) and (35) imply for some $\sigma_3 \geq 0$:

$$\begin{aligned} & \sum_{i=1}^N \|U_i^k - Z^k\|^2 + \|\hat{\nabla} \mathcal{L}(\{U_i^k\}, Z^k, Y_i^k)\|^2 \\ & \leq \sigma_3(\|Z^{k+1} - Z^k\|^2 + \sum_{i=1}^N \|U_i^{k+1} - U_i^k\|^2) \end{aligned} \quad (36)$$

It is noteworthy that we have changed from $\|U_i^{k+1} - Z^{k+1}\|^2$ to $\|U_i^k - Z^k\|^2$. This is because we have proved that $\|U_i^{k+1} - Z^{k+1}\| \rightarrow 0$, which means the gap between these two terms $\|U_i^{k+1} - Z^{k+1}\|^2$ and $\|U_i^k - Z^k\|^2$ are finite. Therefore, we

always can find a finite number $\sigma_3 \geq 0$ to satisfy $\|U_i^k - Z^k\|^2 \leq \sum_{i=1}^N \sigma_3 \|U_i^{k+1} - U_i^k\|^2$. From lemma IV.3, there exists a constant $\sigma_2 = \min\{\frac{L_i}{\rho_i} - \frac{\mu_i}{2}, \mu\}_{i=1}^N$ such that:

$$\begin{aligned} & \mathcal{L}(\{U_i^k\}, Z^k, Y_i^k) - \mathcal{L}(\{U_i^{k+1}\}, Z^{k+1}, Y_i^{k+1}) \\ & \geq \sigma_2(\|Z^{k+1} - Z^k\|^2 + \sum_{i=1}^N \|U_i^{k+1} - U_i^k\|^2) \end{aligned} \quad (37)$$

Combining (36) and (37) we have:

$$\begin{aligned} & \sum_{i=1}^N \|U_i^k - Z^k\|^2 + \|\hat{\nabla} \mathcal{L}(\{U_i^k\}, Z^k, Y_i^k)\|^2 \\ & \leq \frac{\sigma_3}{\sigma_2} (\mathcal{L}(\{U_i^k\}, Z^k, Y_i^k) - \mathcal{L}(\{U_i^{k+1}\}, Z^{k+1}, Y_i^{k+1})) \end{aligned} \quad (38)$$

Summing both sides of the above inequality over $k = 1, \dots, T$. We have the following:

$$\begin{aligned} & \sum_{k=1}^T \left(\sum_{i=1}^N \|U_i^k - Z^k\|^2 + \|\hat{\nabla} \mathcal{L}(\{U_i^k\}, Z^k, Y_i^k)\|^2 \right) \\ & \leq \frac{\sigma_3}{\sigma_2} (\mathcal{L}(\{U_i^1\}, Z^1, Y_i^1) - \mathcal{L}(\{U_i^{T+1}\}, Z^{T+1}, Y_i^{T+1})) \\ & \leq \frac{\sigma_3}{\sigma_2} (\mathcal{L}(\{U_i^1\}, Z^1, Y_i^1) - \underline{\mathcal{L}}) \end{aligned} \quad (39)$$

The last inequality uses the fact that $\mathcal{L}(\{U_i^{T+1}\}, Z^{T+1}, Y_i^{T+1})$ is decreased and lower bounded by $\underline{\mathcal{L}}$ by A.3. By putting $T(\epsilon) := \min\{k | P(\{U_i^k\}, Z^k, Y_i^k) \leq \epsilon, k \geq 0\}$, we can rewrite (39) as follows.

$$T(\epsilon)\epsilon \leq \frac{\sigma_3}{\sigma_2} (\mathcal{L}(\{U_i^1\}, Z^1, Y_i^1) - \underline{\mathcal{L}}) \quad (40)$$

or

$$T(\epsilon) \leq \frac{\sigma_3}{\sigma_2} \frac{(\mathcal{L}(\{U_i^1\}, Z^1, Y_i^1) - \underline{\mathcal{L}})}{\epsilon} \quad (41)$$

This means that for a given ϵ , the proposed algorithm converges with rate of $O(\frac{1}{T(\epsilon)})$. We note that the use of \sum_i^N in the above proof does not mean that we require participation from all clients. This is used to find an upper bound. Let $\beta = \frac{\sigma_3}{\sigma_2}$, theorem IV.8 is achieved.

F. Convergence rates of the proposed methods

Theorem IV.9. Let $T(\epsilon)$ be defined as in Theorem IV.8. Suppose the local update (7) in FedPE is performed using gradient descent with C iterations. Then, the convergence rates for FedPE and FedPG are $O\left(\frac{1}{CT(\epsilon)}\right)$ and $O\left(\frac{1}{C^2T(\epsilon)}\right)$, respectively.

Proof. Based on Theorem IV.8, the general convergence rates of $O(\frac{1}{T(\epsilon)})$ are proved for both FEDPE and FEDPG. While the learning rate of solving problem (15) can be accelerated by using gradient descent on Grassmann manifold with convergence rate of $O(1/C^2)$ [57, Theorem 1], convergence rate for gradient descent on Euclidean space to solve (7) is $O(1/C)$ for strongly convex functions [58]. Therefore, the convergence rates of FEDPE and FEDPG can be estimated as $O(\frac{1}{CT(\epsilon)})$ and $O(\frac{1}{C^2T(\epsilon)})$ respectively.

V. EXPERIMENTAL RESULTS

In this section, we first present the datasets, model settings and measures for performance assessment. Subsequently, to illustrate the efficacy of the proposed methods, we contrast FEDPE and FEDPG with various benchmark strategies within the context of an IDS deployment in IoT networks.

A. Experimental settings

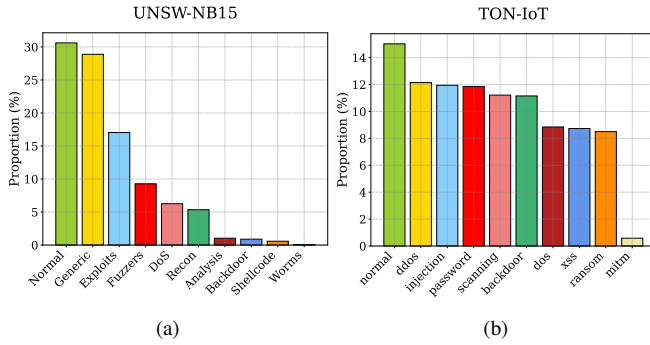


Fig. 3: Class distribution of test sets for UNSW-NB15 and TON-IoT

In our research, all experiments are conducted in a coding environment powered by an AMD Ryzen 3970X Processor with 64 cores and 256GB of RAM. Additionally, four NVIDIA GeForce RTX 3090 GPUs are employed to accelerate the training process. For software, we rely on Python 3 as our primary language, supplemented by advanced machine learning and optimization frameworks such as PyTorch [59] and Scikit-Learn [60]. Our code can be found at: https://github.com/dualgrp/FedPCA_AnomalyDetection.

1) *Datasets and Metrics*: In this study, we employ the UNSW-NB15 [13] and TON-IoT Network [14] datasets. The former, a benchmark in network intrusion detection system (NIDS) research, encompasses a myriad of network traffic scenarios, with various attack types interlaced with normal activities commonly found in real-world network (internet) environments. The latter, TON-IoT, includes heterogeneous data sourced from Telemetry datasets of IoT and IIoT sensors, amassed through parallel processing to capture a spectrum of normal and cyber-attack events. Following preprocessing, from the UNSW-NB15 dataset, we utilized a training set of 56,000 normal samples and a test set comprising 20,000 normal and 45,332 abnormal samples, all with 39 numerical features. From the TON-IoT dataset, our training set consists of 114,956 normal samples, while the test set includes 10,000 normal samples and 56,557 abnormal samples, all with 49 numerical features. The class distribution of the test sets for both datasets is illustrated in Fig.3a and Fig.3b respectively. These carefully selected and prepared datasets serve as a solid foundation for the evaluation of our proposed approach.

In the setting of a host-based ML-IDS deployment, each IoT device functions as a localized ML-IDS, using its unique data to develop an anomaly detection model. This approach reflects the inherent diversity of traffic distribution across disparate clients, and to mimic this realistically, the comprehensive training set is equally subdivided into 100 individual client datasets,

each representing non-identically distributed (non-i.i.d.) local data. This subdivision is achieved by grouping records based on the number of connections that contain the same service (*ct_srv_src*) for UNSW-NB15 and the range of source ports (*srcports*) for TON-IoT.

2) *Baselines*: In order to highlight the efficacy of FEDPE and FEDPG in IoT network anomaly detection, we conduct a comprehensive comparative study against a variety of unsupervised techniques including:

- Self-learning PCA*: a stand-alone method where each client individually learns its PCA matrix using only its local dataset. By identifying the principal patterns within this dataset, anomalies are detected when there's a substantial discrepancy between the original data and its PCA-reconstructed version.
- AutoEncoder (AE)*: an unsupervised learning method constructed of an encoder and a decoder in the form of neural networks. AE facilitates anomaly detection by compressing input data during encoding and then attempting to reconstruct it. Anomalies are identified when there's a notable difference between the input data and its reconstructed version, suggesting the input doesn't conform to typical patterns within the dataset [6].
- Bidirectional Generative Adversarial Network (BiGAN)*: a generative model composed of a generator, a discriminator and an encoder. During BiGAN's adversarial training, the encoder maps real data into latent representations. The generator then tries to recreate data from these representations, aiming to closely match the original input. Concurrently, the discriminator distinguishes between pairs of real data and their latent encodings, and the output from the generator with its corresponding latent representations. When trained solely on normal data, BiGAN can detect anomalies by noting high reconstruction errors, which indicate deviations from the learned representations of normal data [7], [8].

We subsequently employ the de-facto FedAvg [16] to ensure consistency in the training of AE and BiGAN within federated settings. In line with this, we establish FedAE and FedBiGAN – which utilize two-layer neural networks for their components, and FedAE-2 and FedBiGAN-2 – which incorporate four-layer neural networks for more complex non-linear structures. For Self-learning PCA, we train a distinct PCA matrix tailored for each client's dataset and then assess the average performance across all clients on detecting anomalies on the test set. The selection of these baseline models, widely acclaimed in the field and each offering distinct methodologies for anomaly detection, ensures a robust evaluation of our methods against diverse unsupervised paradigms.

3) *Performance Metrics*: In this work, we are primarily concerned with identifying anomalies in network traffic. Hence, the main metrics employed are:

- Accuracy**: calculates the ratio of correctly identified both normal and anomalies to the total instances in the dataset, offering a general perspective on the model performance.
- Precision**: represents the ratio of true anomalies to all detections labeled as anomalies, assessing the exactness of the identified anomalies.

- 3) **Recall**: quantifies the proportion of actual anomalies that are correctly flagged by the detection system, assessing the ability of a model to capture all potential threats.
- 4) **F1-Score**: calculates the harmonic mean of precision and recall, underscoring the balance between the detection of true anomalies and the risk of false alarms.
- 5) **False Negative Rate (FNR)**: Represents the fraction of actual anomalies that are incorrectly flagged as normal.
- 6) **Area Under the Receiver Operating Characteristic curve (AUC-ROC)**: A graphical representation plotting True Positive Rate (TPR) against False Positive Rate (FPR) across varying threshold settings, furnishing a comprehensive performance overview.
- 7) **Precision-Recall (PR) curves**: Serving as a visual instrument to gauge the relationship between precision and recall, this becomes vital, particularly in imbalanced datasets where anomalies are few.

4) *Training Details*: To provide a practical test for our proposed methods, we train our federated PCA models on each client's dataset, without inter-client data sharing. The comprehensive testing set, inclusive of unknown attacks, is applied uniformly to all methods. Preceding training, all features undergo normalization through a z-score function, utilizing the standard deviation and mean values calculated from the corresponding training set. The following experiments have hyperparameters fine-tuned via a grid search to ensure optimal test performance. Furthermore, each communication round includes a randomly selected subset of clients, constituting 10% of the total count, replicating real-world scenarios where not all devices might be available for communication simultaneously.

B. Experimental Results

1) *Efficiency of Federated PCA on Grassmann Manifold*: In our analysis, we scrutinize the convergence efficacy of our Federated PCA algorithms — FEDPE (Federated PCA over Euclidean Space) and FEDPG (Federated PCA over Grassmann Manifold) — as depicted in Fig.4, Fig. 6 and Fig. 5. Notably, for the same number of local communication rounds ($LE = 10$), FedPG displays a significantly faster convergence compared to FedPE. It's worth noting that FEDPE can achieve quicker convergence by augmenting the value of LE , although this also extends the training duration. These findings underscore FEDPG's ability to deliver robust detection performance with decreased training time, an attribute highly sought after in practical IDS development contexts. Fig.4a, 4b illustrate the precise performance of FEDPG across various thresholds. In our study, we uniformly set $\rho = 1.0$ across all methods and investigate their detection performance by various metrics.

The impact of low-rank approximation is presented in Fig. 5a and 5b. Surprisingly, increasing the rank-k does not necessarily lead to an improvement in the performance of both FEDPG and FEDPE, as observed in both datasets. This suggests that our PCA-based anomaly detection algorithms can maintain a low memory footprint and operate efficiently with low computational complexity, making them ideal for resource-constrained environments. Despite FEDPG and FEDPE providing better approximations for a given dataset with larger rank-k,

they also tend to precisely recover data points lying in high-dimensional space. However, high-dimensional data samples often act as outliers, resembling attacks at times. This creates a dilemma between achieving optimal performance and accurate approximation, as seen in the loss-accuracy contrast presented in Fig. 5c, 5d, and Fig. 5a, 5b. Abnormal detection using PCA relies on measuring the distance between data points and principal components, making it challenging to differentiate between high-dimensional data points and malicious data.

To examine the effectiveness of FEDPG against FEDPE in terms of computational complexity, we investigate the training time of both algorithms on the same machine. While Fig. 6a and 6c demonstrate that FEDPE surpasses FEDPG in terms of the total number of communication rounds, our investigation reveals that FEDPG is more effective in managing computational costs, as depicted in Fig. 6b and 6d. It is worth noting that FEDPG sacrifices a small amount of computational resources in exchange for significantly higher performance.

2) *Effects of number clients on performance*: We evaluate the performance of FEDPE and FEDPG on different scales of IoT systems by varying the number of clients. The results illustrated in Fig. 7 reveal a noticeable trade-off between training time and accuracy for these algorithms.

For both datasets, FEDPG consistently demonstrated a significantly shorter training time as compared to FEDPE, regardless of the number of clients. For example, on the TON-IoT dataset, the training time of FEDPG was less than a sixth of the training time of FEDPE for the same number of clients. In contrast, the accuracy of FEDPG remained relatively constant and independent of the number of clients in both datasets. FEDPE, on the other hand, demonstrated an improvement in accuracy as the number of clients increased. However, even with this improvement, it was unable to reach the accuracy of FEDPG on the TON-IoT dataset. For the UNSW-NB15 dataset, both algorithms performed comparably in terms of accuracy, with FEDPE even slightly surpassing FEDPG in fewer clients, but then slightly underperforming in more clients.

These results suggest that FEDPG could offer substantial time savings over FEDPE without compromising detection accuracy, particularly for large numbers of clients. However, the appropriate choice of algorithm may also depend on the specific requirements and constraints of the task and system at hand, such as the importance of speed versus detection accuracy and the number of clients in the system.

3) *Performance of Network Anomaly Detection Tasks*: We evaluate the performance of FEDPG alongside other baselines in the context of network anomaly detection on both the UNSW-NB15 and TON-IoT datasets. For all methods, we establish optimal thresholds to delineate normal from anomalous behavior using the AUC-ROC curve corresponding to their reconstruction errors. This approach aims to strike a balance by maximizing TPR and minimizing FPR, ensuring robustness and precision in anomaly detection. Such an evidence-driven thresholding strategy underscores the reliability of the reconstruction error as a metric for detecting anomalies in network traffic.

As indicated in Table I, Self-learning PCA, while offering a foundational unsupervised technique, lags behind in performance when compared to other methods. This outcome aligns

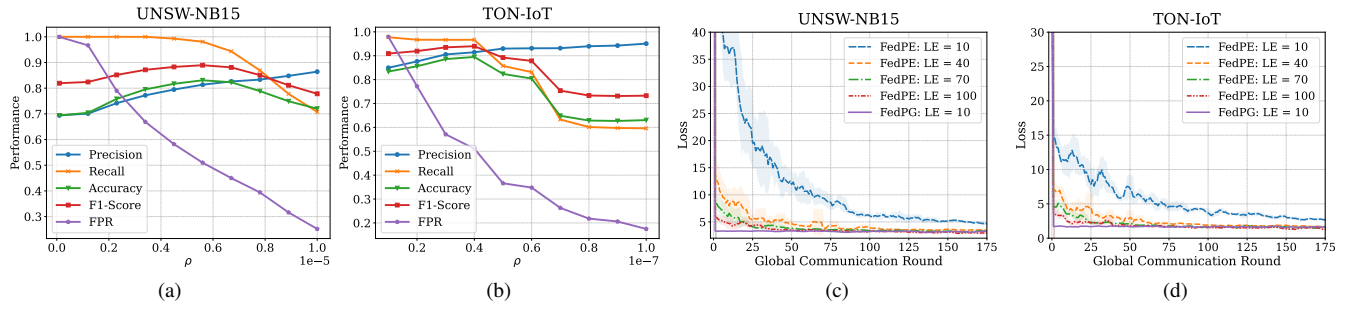
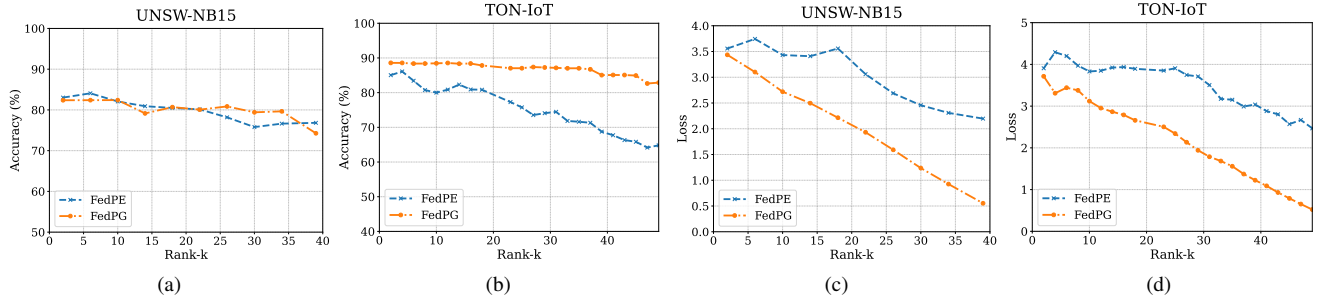
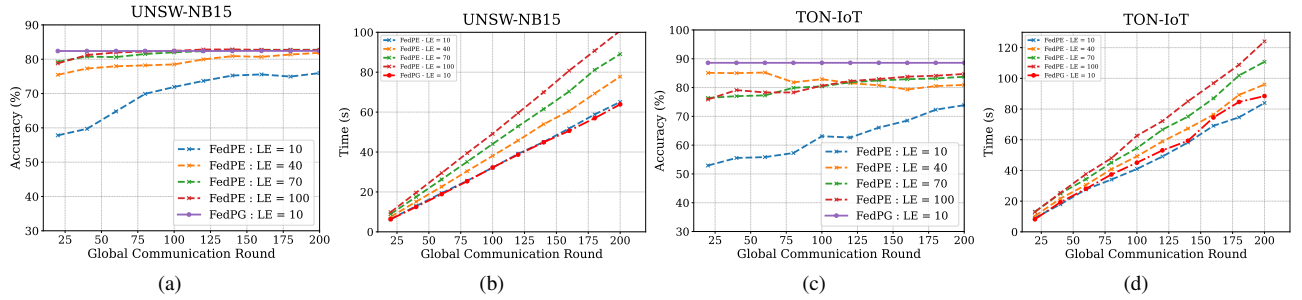
Fig. 4: (a,b) Effects of ρ on the performance of FEDPG and (c,d) Training loss over global iterationsFig. 5: Effects of rank- k on the performance of FEDPE and FEDPG

Fig. 6: Test accuracy and training time over global iterations of FEDPE and FEDPG on UNSW-NB15 (a,b) and TON-IoT (c,d)

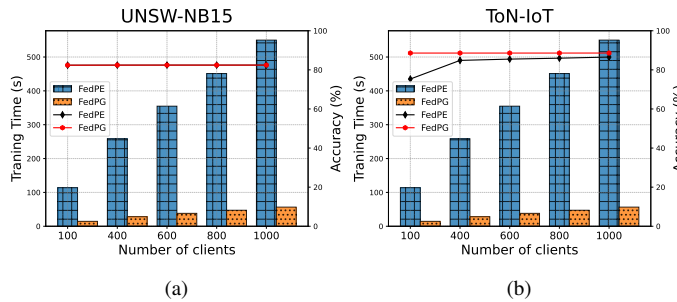


Fig. 7: Effects of number of clients on training time and performance of FEDPE and FEDPG

with expectations, given the diverse and highly heterogeneous nature of clients' data. The performance of FEDPG and FEDPE is comparable and slightly better than FedAE and FedBiGAN. Additionally, they demonstrate a competitive performance against more sophisticated non-linear structures such as FedAE-2 and FedBiGAN-2. It should be noted that while FEDPG may not outperform all other techniques across all metrics, it does exhibit a commendable balance of measures.

On the UNSW-NB15 dataset, FEDPG not only shows a high accuracy (81.95%) but also balances this with a relatively low false negative rate (6.63%), indicating a robust ability to correctly classify normal behavior while minimizing the chance of missing true anomalies. Similarly, on TON-IoT, FEDPG holds its own by showcasing the highest recall (94.32%), reflecting its superior ability to correctly identify anomalous events. Moreover, it has the lowest false negative rate (5.68%) among the evaluated methods, which underscores its performance stability. Furthermore, the linear nature of FEDPG simplifies model interpretability, often leading to more computationally and communication-efficient solutions while still being able to capture significant patterns in the data for network anomaly detection. Meanwhile, although FedAE, FedAE-2, FedBiGAN, and FedBiGAN-2 can potentially capture more complex relationships in the data, they tend to require more computational and memory resources, harder to interpret and may not always result in better performance. This suggests that the balanced performance of our linear method FEDPG is an attractive alternative for real-world IDS where simplicity, efficiency, and interpretability are crucial.

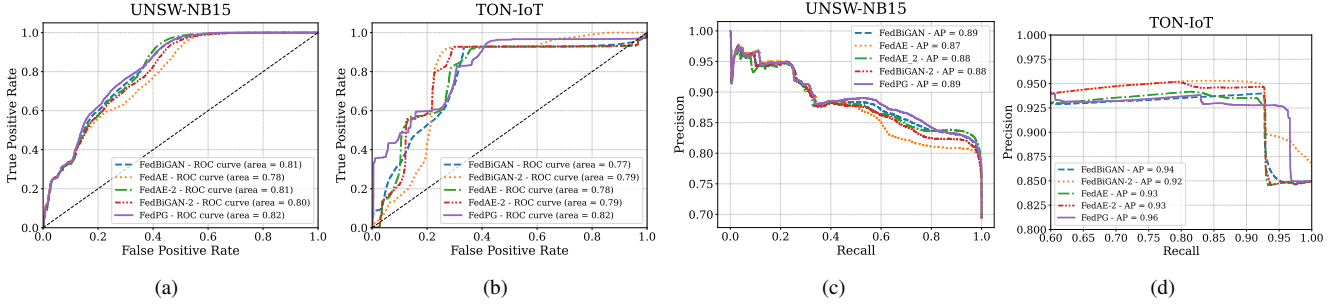


Fig. 8: (a,b) Receiver Operating Characteristic (ROC) curve and (c,d) Precision-Recall curve

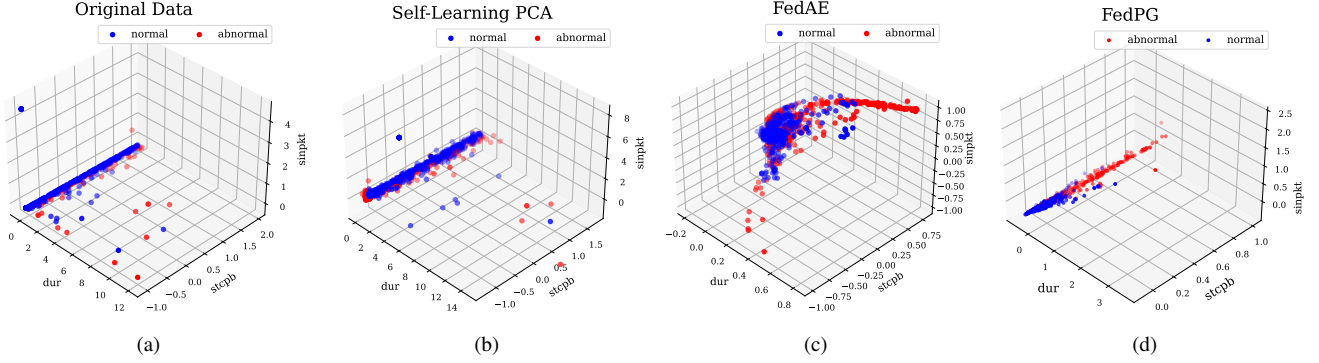


Fig. 9: Visualization of UNSW-NB15 traffic after reconstruction using different methods

TABLE I: Performance of network anomaly detection tasks on UNSW-NB15 and TON-IoT datasets.

Dataset	UNSW-NB15					TON-IoT					
	Method	Acc	Pre	Recall	F1-Score	FNR	Acc	Pre	Recall	F1-Score	FNR
Self-learning PCA		63.80	83.19	59.94	69.68	40.06	51.81	86.79	51.07	64.30	48.93
FedAE		80.88	80.66	95.27	87.36	4.73	87.28	93.52	91.36	92.43	8.64
FedAE-2		82.80	83.45	93.80	88.32	6.20	89.09	94.68	92.34	93.50	7.66
FedBiGAN		81.21	83.04	91.63	87.12	8.36	88.53	93.98	92.42	93.19	7.57
FedBiGAN-2		81.59	81.98	94.16	87.65	5.84	89.08	95.05	91.93	93.47	8.07
FEDPE (ours)		82.15	81.06	95.14	87.53	6.25	87.06	89.82	94.94	92.31	6.13
FEDPG (ours)		81.95	82.82	93.36	87.77	6.63	88.94	92.79	94.32	93.55	5.68

The superior performance of FEDPG is further validated by the area under the Receiver Operating Characteristic (AUC-ROC) and Precision-Recall curves, depicted in Fig. 8. On both the UNSW-NB15 and TON-IoT datasets, FEDPG demonstrates higher AUC-ROC values of 0.82, surpassing other baselines (Fig. 8a, 8b), indicating its enhanced ability to maintain high true positive rates while reducing false positive rates. This performance superiority is corroborated by the Precision-Recall curves, with FEDPG achieving an Average Precision (AP) of 0.89 and 0.96 on UNSW-NB15 and TON-IoT datasets respectively (Fig. 8c, 8d), comparable with the competing methods. These results collectively affirm the robustness of FEDPG in achieving high precision at various levels of recall, underscoring its potential as an effective solution for network anomaly detection.

To delve deeper into the efficacy of the suggested technique, we employed 3D scatter plots to illustrate the transformation of UNSW-NB15 traffic logs as per the techniques described, as depicted in Fig.9. For the purpose of plotting, we chose

three features¹, following which we reconstructed the original logs from the latent representation discerned by Self-Learning PCA, FedAE, and FEDPG. It's evident that FEDPG essentially repositions original logs from an established coordinate framework into an alternate one, proficient in distinguishing between regular logs and anomalies. This affirms that when FEDPG redevelops the original logs from the primary components, it results in a minimal reconstruction discrepancy for regular data but a substantial error.

4) *Communication Efficiency*: In the realm of IoT anomaly detection, the transmission size of models during communication rounds plays a pivotal role, directly influencing bandwidth and overall efficiency. Our study reveals a significant communication advantage of FEDPG when juxtaposed against FedAE, FedBiGAN, FedAE-2, and FedBiGAN-2. Specifically, when considering the UNSW-NB15 datasets, FEDPG boasts a communication efficiency that's 6.7 and 10 times superior

¹ Network features in Fig.9: duration ('dur'), source TCP base sequence number ('stcpb'), source interpacket arrival time ('sinpkt')

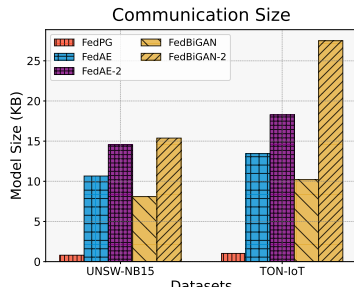


Fig. 10: The size of model exchanged in each communication round.

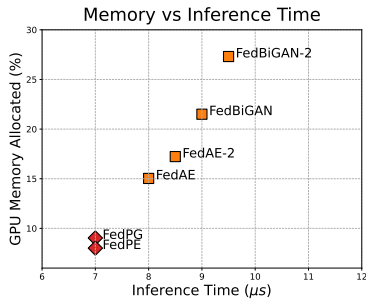


Fig. 11: The memory consumption and inference time of all methods.

to FedAE and FedBiGAN respectively. While FedAE-2 and FedBiGAN-2 may have a slight edge performance-wise, their demand for bandwidth is significantly higher, necessitating model sizes 10 and 15 times that of FEDPG. A similar efficiency is observed for the TON-IoT dataset, where FEDPG outperforms by factors of up to 20 times compared to other methods. These results hold considerable significance in the context of FL, where the reduction of bandwidth utilization is a paramount concern. This evidence underscores the ability of FEDPG to strike an effective balance between reliable anomaly detection and optimal resource usage, thus bolstering its suitability for real-world NIDS applications.

5) *Memory and Time Complexity*: We analyze all models through the lens of GPU memory consumption (measured in a percentage) and wall-clock time for inference (measured in a microsecond - μs), a perceptible trade-off emerges between these two metrics. As depicted in Fig. 11, FEDPG and FEDPE are relatively memory-efficient, consuming around 9.03% and 8.01% of GPU memory during training, respectively. In contrast, the more sophisticated models, FedAE, FedAE-2, FedBiGAN, and FedBiGAN-2, are more resource-demanding, utilizing larger amounts of memory. Despite the smaller memory footprint, FEDPG and FEDPE do not compromise on the inference speed, clocking an impressive inference wall-clock time of approximately $7\mu\text{s}$. This slightly outperforms the inference time taken by other non-linear methods. Thus, the superior balance struck by FEDPG and FEDPE between GPU memory usage and wall-clock time solidifies their efficiency, making them well-suited for resource-restricted environments.

VI. CONCLUSION

In this study, we analyze the convergence of the federated PCA framework on the Grassmann manifold, thereby enhancing

efficient unsupervised anomaly detection in IoT networks with realistic datasets. The proposed framework empowers IoT devices to collaboratively create a profile of normal network traffic while abstaining from the exchange of local data. Specifically, we devise FEDPE, an innovative federated algorithm that approximates PCA utilizing the principle of ADMM and is accompanied by theoretical guarantees. We further conceptualize the federated PCA via Grassmannian optimization and propose another algorithm, FEDPG. This algorithm is geared towards ensuring a swift training process and early anomaly detection, even within computing environments that are resource-constrained. Through our experimental evaluations, we establish the adaptability of FEDPE and FEDPG to the IoT environment and demonstrate their superior performance over conventional approaches when tested on the UNSW-NB15 and TON-IoT datasets.

REFERENCES

- [1] A. Zanella, N. Bui, A. Castellani, L. Vangelista, and M. Zorzi, "Internet of things for smart cities," *IEEE Internet of Things Journal*, vol. 1, no. 1, pp. 22–32, 2014.
- [2] X. Yang, P. Zhao, X. Zhang, J. Lin, and W. Yu, "Toward a gaussian-mixture model-based detection scheme against data integrity attacks in the smart grid," *IEEE Internet of Things Journal*, vol. 4, no. 1, pp. 147–161, 2016.
- [3] Z. Afroz, G. Shafullah, T. Urmee, and G. Higgins, "Modeling techniques used in building hvac control systems: A review," *Renewable and sustainable energy reviews*, vol. 83, pp. 64–84, 2018.
- [4] A. A. Cook, G. Misirli, and Z. Fan, "Anomaly detection for iot time-series data: A survey," *IEEE Internet of Things Journal*, vol. 7, no. 7, pp. 6481–6494, 2019.
- [5] D. Chou and M. Jiang, "A survey on data-driven network intrusion detection," *ACM Comput. Surv.*, vol. 54, no. 9, oct 2021.
- [6] C. Ieracitano, A. Adeel, F. C. Morabito, and A. Hussain, "A novel statistical analysis and autoencoder driven intelligent intrusion detection approach," *Neurocomputing*, vol. 387, pp. 51–62, 2020.
- [7] H. Zenati, C.-S. Foo, B. Lecouat, G. Manek, and V. R. Chandrasekhar, "Efficient gan-based anomaly detection," *ArXiv*, vol. abs/1802.06222, 2018.
- [8] H. Zenati, M. Romain, C. Foo, B. Lecouat, and V. Chandrasekhar, "Adversarially learned anomaly detection," in *2018 IEEE International Conference on Data Mining (ICDM)*. Los Alamitos, CA, USA: IEEE Computer Society, nov 2018, pp. 727–736.
- [9] L. Ruff, J. R. Kauffmann, R. A. Vandermeulen, G. Montavon, W. Samek, M. Kloft, T. G. Dietterich, and K.-R. Muller, "A Unifying Review of Deep and Shallow Anomaly Detection," *Proceedings of the IEEE*, vol. 109, no. 5, pp. 756–795, May 2021.
- [10] B. Schölkopf, J. Platt, and T. Hofmann, *In-Network PCA and Anomaly Detection*, 2007, pp. 617–624.
- [11] S. Boyd, N. Parikh, E. Chu, B. Peleato, J. Eckstein *et al.*, "Distributed optimization and statistical learning via the alternating direction method of multipliers," *Foundations and Trends® in Machine learning*, vol. 3, no. 1, pp. 1–122, 2011.
- [12] T.-A. Nguyen, J. He, L. T. Le, W. Bao, and N. H. Tran, "Federated pca on grassmann manifold for anomaly detection in iot networks," in *IEEE INFOCOM 2023 - IEEE Conference on Computer Communications*, 2023, pp. 1–10.
- [13] N. Moustafa and J. Slay, "Unsw-nb15: a comprehensive data set for network intrusion detection systems (unsw-nb15 network data set)," in *2015 Military Communications and Information Systems Conference (MilCIS)*, 2015, pp. 1–6.
- [14] T. M. Booij, I. Chiscop, E. Meeuwissen, N. Moustafa, and F. T. H. d. Hartog, "Ton_iot: The role of heterogeneity and the need for standardization of features and attack types in iot network intrusion data sets," *IEEE Internet of Things Journal*, vol. 9, no. 1, pp. 485–496, 2022.
- [15] J. Konecný, H. B. McMahan, and D. Ramage, "Federated optimization: Distributed optimization beyond the datacenter," *ArXiv*, vol. abs/1511.03575, 2015.

[16] B. McMahan, E. Moore, D. Ramage, S. Hampson, and B. A. y. Arcas, "Communication-Efficient Learning of Deep Networks from Decentralized Data," in *Proceedings of the 20th International Conference on Artificial Intelligence and Statistics*, ser. Proceedings of Machine Learning Research, A. Singh and J. Zhu, Eds., vol. 54. PMLR, 20–22 Apr 2017, pp. 1273–1282.

[17] D. C. Nguyen, M. Ding, P. N. Pathirana, A. Seneviratne, J. Li, and H. V. Poor, "Federated learning for internet of things: A comprehensive survey," *IEEE Communications Surveys & Tutorials*, vol. 23, no. 3, pp. 1622–1658, 2021.

[18] J. Konečný, H. B. McMahan, F. X. Yu, P. Richtárik, A. T. Suresh, and D. Bacon, "Federated Learning: Strategies for Improving Communication Efficiency," *arXiv:1610.05492 [cs]*, Oct. 2017.

[19] A. T. Suresh, F. X. Yu, S. Kumar, and H. B. McMahan, "Distributed mean estimation with limited communication," in *Proceedings of the 34th International Conference on Machine Learning*, ser. Proceedings of Machine Learning Research, D. Precup and Y. W. Teh, Eds., vol. 70. PMLR, 06–11 Aug 2017, pp. 3329–3337.

[20] A. Reisizadeh, A. Mokhtari, H. Hassani, A. Jadbabaie, and R. Pedarsani, "Fedpac: A communication-efficient federated learning method with periodic averaging and quantization," in *Proceedings of the Twenty Third International Conference on Artificial Intelligence and Statistics*, ser. Proceedings of Machine Learning Research, S. Chiappa and R. Calandra, Eds., vol. 108. PMLR, 26–28 Aug 2020, pp. 2021–2031.

[21] F. Sattler, S. Wiedemann, K.-R. Müller, and W. Samek, "Robust and communication-efficient federated learning from non-i.i.d. data," *IEEE Transactions on Neural Networks and Learning Systems*, vol. 31, no. 9, pp. 3400–3413, 2020.

[22] Y. Wang, L. Lin, and J. Chen, "Communication-efficient adaptive federated learning," in *Proceedings of the 39th International Conference on Machine Learning*, ser. Proceedings of Machine Learning Research, K. Chaudhuri, S. Jegelka, L. Song, C. Szepesvari, G. Niu, and S. Sabato, Eds., vol. 162. PMLR, 17–23 Jul 2022, pp. 22802–22838.

[23] Y. Zhao, M. Li, L. Lai, N. Suda, D. Civin, and V. Chandra, "Federated Learning with Non-IID Data," *arXiv:1806.00582 [cs, stat]*, Jun. 2018.

[24] X. Li, K. Huang, W. Yang, S. Wang, and Z. Zhang, "On the Convergence of FedAvg on Non-IID Data," *arXiv:1907.02189*, Jun. 2020.

[25] J. Zhang, G. Zhu, R. W. Heath Jr, and K. Huang, "Grassmannian learning: Embedding geometry awareness in shallow and deep learning," *arXiv:1808.02229*, 2018.

[26] Z. Huang, J. Wu, and L. Van Gool, "Building deep networks on grassmann manifolds," in *Proceedings of the Thirty-Second AAAI Conference on Artificial Intelligence and Thirtieth Innovative Applications of Artificial Intelligence Conference and Eighth AAAI Symposium on Educational Advances in Artificial Intelligence*, 2018.

[27] B. Wang, Y. Hu, J. Gao, Y. Sun, H. Chen, M. Ali, and B. Yin, "Locality preserving projections for grassmann manifold," in *Proceedings of the Twenty-Sixth International Joint Conference on Artificial Intelligence (IJCAI-17)*, Aug. 2017, pp. 2893–2900.

[28] Z. Huang, R. Wang, S. Shan, and X. Chen, "Projection metric learning on grassmann manifold with application to video based face recognition," in *2015 IEEE Conference on Computer Vision and Pattern Recognition (CVPR)*, June 2015, pp. 140–149.

[29] N. Neshenko, E. Bou-Harb, J. Crichigno, G. Kaddoum, and N. Ghani, "Demystifying iot security: An exhaustive survey on iot vulnerabilities and a first empirical look on internet-scale iot exploitations," *IEEE Communications Surveys & Tutorials*, vol. 21, no. 3, 2019.

[30] Y. Meidan, M. Bohadana, Y. Mathov, Y. Mirsky, A. Shabtai, D. Breitenbacher, and Y. Elovici, "N-baito—network-based detection of iot botnet attacks using deep autoencoders," *IEEE Pervasive Computing*, vol. 17, no. 3, pp. 12–22, 2018.

[31] E. Anthi, L. Williams, M. Słowińska, G. Theodorakopoulos, and P. Burnap, "A supervised intrusion detection system for smart home iot devices," *IEEE Internet of Things Journal*, vol. 6, no. 5, 2019.

[32] H. H. Pajouh, R. Javidan, R. Khayami, A. Dehghanianha, and K.-K. R. Choo, "A two-layer dimension reduction and two-tier classification model for anomaly-based intrusion detection in iot backbone networks," *IEEE Transactions on Emerging Topics in Computing*, vol. 7, no. 2, 2019.

[33] M. Zolanvari, M. A. Teixeira, L. Gupta, K. M. Khan, and R. Jain, "Machine learning-based network vulnerability analysis of industrial internet of things," *IEEE Internet of Things Journal*, vol. 6, no. 4, pp. 6822–6834, 2019.

[34] N. Wang, Y. Chen, Y. Hu, W. Lou, and Y. T. Hou, "Manda: On adversarial example detection for network intrusion detection system," in *IEEE INFOCOM 2021 - IEEE Conference on Computer Communications*, 2021, pp. 1–10.

[35] H. Qiu, T. Dong, T. Zhang, J. Lu, G. Memmi, and M. Qiu, "Adversarial attacks against network intrusion detection in iot systems," *IEEE Internet of Things Journal*, vol. 8, no. 13, pp. 10327–10335, 2021.

[36] T. D. Nguyen, S. Marchal, M. Miettinen, H. Fereidooni, N. Asokan, and A.-R. Sadeghi, "Diot: A federated self-learning anomaly detection system for iot," in *IEEE International Conference on Distributed Computing Systems (ICDCS)*, 2019, pp. 756–767.

[37] N. Wang, Y. Chen, Y. Hu, W. Lou, and Y. T. Hou, "Feco: Boosting intrusion detection capability in iot networks via contrastive learning," in *IEEE INFOCOM 2022 - IEEE Conference on Computer Communications*, 2022, pp. 1409–1418.

[38] V. Mothukuri, P. Khare, R. M. Parizi, and et al., "Federated-learning-based anomaly detection for iot security attacks," *IEEE Internet of Things Journal*, vol. 9, no. 4, pp. 2545–2554, 2021.

[39] I. Jolliffe, *Principal Component Analysis*. John Wiley & Sons, Ltd, 2014. [Online]. Available: <https://onlinelibrary.wiley.com/doi/abs/10.1002/9781118445112.stat006472>

[40] A. Lakhina, M. Crovella, and C. Diot, "Diagnosing network-wide traffic anomalies," *ACM SIGCOMM computer communication review*, vol. 34, no. 4, pp. 219–230, 2004.

[41] D. Brauckhoff, K. Salamatian, and M. May, "Applying pca for traffic anomaly detection: Problems and solutions," in *IEEE INFOCOM 2009*, 2009, pp. 2866–2870.

[42] J. Chen, S. Yin, S. Cai, L. Zhao, and S. Wang, "L-kpca: an efficient feature extraction method for network intrusion detection," in *17th International Conference on Mobility, Sensing and Networking (MSN)*, 2021, pp. 683–684.

[43] S. X. Wu, H.-T. Wai, L. Li, and A. Scaglione, "A review of distributed algorithms for principal component analysis," *Proceedings of the IEEE*, vol. 106, no. 8, pp. 1321–1340, 2018.

[44] J. Ge, Z. Wang, M. Wang, and H. Liu, "Minimax-optimal privacy-preserving sparse pca in distributed systems," in *Proceedings of the Twenty-First International Conference on Artificial Intelligence and Statistics*, vol. 84. PMLR, 09–11 Apr 2018, pp. 1589–1598.

[45] A. Grammenos, R. Mendoza Smith, J. Crowcroft, and C. Mascolo, "Federated principal component analysis," *Advances in Neural Information Processing Systems*, vol. 33, pp. 6453–6464, 2020.

[46] J. Giesen and S. Laue, "Distributed convex optimization with many convex constraints," *arXiv preprint arXiv:1610.02967*, 2016.

[47] M. Hong, Z.-Q. Luo, and M. Razaviyayn, "Convergence analysis of alternating direction method of multipliers for a family of nonconvex problems," in *2015 IEEE International Conference on Acoustics, Speech and Signal Processing (ICASSP)*, 2015, pp. 3836–3840.

[48] T.-H. Chang, W.-C. Liao, M. Hong, and X. Wang, "Asynchronous distributed admm for large-scale optimization—part ii: Linear convergence analysis and numerical performance," *IEEE Transactions on Signal Processing*, vol. 64, no. 12, pp. 3131–3144, 2016.

[49] M. Hong, Z.-Q. Luo, and M. Razaviyayn, "Convergence analysis of alternating direction method of multipliers for a family of nonconvex problems," *SIAM Journal on Optimization*, vol. 26, no. 1, pp. 337–364, 2016.

[50] X. Zhang, M. M. Khalili, and M. Liu, "Improving the privacy and accuracy of ADMM-based distributed algorithms," in *Proceedings of the 35th International Conference on Machine Learning*, ser. Proceedings of Machine Learning Research, J. Dy and A. Krause, Eds., vol. 80. PMLR, 10–15 Jul 2018, pp. 5796–5805.

[51] A. Elgabli, J. Park, S. Ahmed, and M. Bennis, "L-fgadmm: Layer-wise federated group admm for communication efficient decentralized deep learning," *2020 IEEE Wireless Communications and Networking Conference (WCNC)*, pp. 1–6, 2019.

[52] S. Zhou and G. Y. Li, "Communication-efficient admm-based federated learning," *CoRR*, vol. abs/2110.15318, 2021.

[53] S. Yue, J. Ren, J. Xin, S. Lin, and J. Zhang, "Inexact-admm based federated meta-learning for fast and continual edge learning," in *Proceedings of the Twenty-Second International Symposium on Theory, Algorithmic Foundations, and Protocol Design for Mobile Networks and Mobile Computing*, ser. MobiHoc '21. New York, NY, USA: Association for Computing Machinery, 2021, p. 91–100.

[54] I. T. Jolliffe, *Principal component analysis for special types of data*. Springer, 2002.

[55] M. Udell, C. Horn, R. Zadeh, and S. Boyd, "Generalized low rank models," *Foundations and Trends® in Machine Learning*, vol. 9, no. 1, pp. 1–118, 2016.

[56] S. Boyd, N. Parikh, E. Chu, B. Peleato, and J. Eckstein, "Distributed optimization and statistical learning via the alternating direction method of multipliers," *Foundations and Trends® in Machine Learning*, vol. 3, no. 1, pp. 1–122, 2011.

- [57] L. Lin, B. Saparbayeva, M. M. Zhang, and D. B. Dunson, "Accelerated algorithms for convex and non-convex optimization on manifolds," *arXiv preprint arXiv:2010.08908*, 2020.
- [58] S. Bubeck *et al.*, "Convex optimization: Algorithms and complexity," *Foundations and Trends® in Machine Learning*, vol. 8, no. 3-4, pp. 231–357, 2015.
- [59] A. Paszke, S. Gross, S. Chintala, G. Chanan, E. Yang, Z. DeVito, Z. Lin, A. Desmaison, L. Antiga, and A. Lerer, "Automatic differentiation in pytorch," in *NIPS 2017 Workshop on Autodiff*, 2017. [Online]. Available: <https://openreview.net/forum?id=BJJsrmfCZ>
- [60] F. Pedregosa, G. Varoquaux, A. Gramfort, V. Michel, B. Thirion, O. Grisel, M. Blondel, P. Prettenhofer, R. Weiss, V. Dubourg *et al.*, "Scikit-learn: Machine learning in python," *Journal of machine learning research*, vol. 12, no. Oct, pp. 2825–2830, 2011.

VII. BIOGRAPHY SECTION



Tung-Anh Nguyen received his B.E. degree in Electronics and Telecommunications from Hanoi University of Science and Technology (HUST), Vietnam, in 2016. He received his MSc degree in Computer and Information Science from Korea University, Korea, in 2019. Currently, he is pursuing a PhD degree in Computer Science at DUAL group, Faculty of Engineering, the University of Sydney (USyd), NSW, Australia. His research interests include Distributed Machine Learning, Federated Learning, Blockchain and Optimization for Distributed Systems.



Long Tan Le received B.E. degree with honours in Computer Engineering from Ho Chi Minh City University of Technology (HCMUT) in 2018. He was a researcher at the Faculty of Computer Science and Engineering, HCMUT from 2018 to 2021. Currently, he is pursuing a Ph.D. degree in Computer Science at the Faculty of Engineering, the University of Sydney (USyd). His research interests include Machine Learning, Federated Learning, and their applications for next-generation networking.



Tuan Dung Nguyen received his B.S. from the University of Melbourne and M.Phil. from the Australian National University, both in computer science. He is currently pursuing a Ph.D. in computer and information science at the University of Pennsylvania, where he is a part of the Computational Social Science Lab. His research interests span machine learning, convex optimization, distributed computing and social network analysis.



Wei Bao (Member, IEEE) received the BE degree in communications engineering from the Beijing University of Posts and Telecommunications, Beijing, China, in 2009, the MSc degree in electrical and computer engineering from the University of British Columbia, Vancouver, Canada, in 2011, and the PhD degree in electrical and computer engineering from the University of Toronto, Toronto, Canada, in 2016. He is currently a senior lecturer with the School of Computer Science, University of Sydney, Sydney, Australia. His research covers the area of network science, with particular emphasis on Internet of things, mobile computing, edge computing, and distributed learning. He received the Best Paper Awards in ACM International Conference on Modeling, Analysis and Simulation of Wireless and Mobile Systems (MSWiM) in 2013 and 2019 and IEEE International Symposium on Network Computing and Applications (NCA) in 2016.



Suranga Seneviratne (Senior Member, IEEE) received the bachelor's degree from University of Moratuwa, Sri Lanka, in 2005, and the Ph.D. degree from University of New South Wales, Australia, in 2015. He is a Lecturer of Security with the School of Computer Science, The University of Sydney. His current research interests include privacy and security in mobile systems, AI applications in security, and behavior biometrics. Before moving into research, he worked nearly six years in the telecommunications industry in core network planning and operations



Choong Seon Hong (S'95-M'97-SM'11) received the B.S. and M.S. degrees in electronic engineering from Kyung Hee University, Seoul, South Korea, in 1983 and 1985, respectively, and the Ph.D. degree from Keio University, Tokyo, Japan, in 1997. In 1988, he joined KT, Gyeonggi-do, South Korea, where he was involved in broadband networks as a member of the Technical Staff. Since 1993, he has been with Keio University. He was with the Telecommunications Network Laboratory, KT, as a Senior Member of Technical Staff and as the Director of the Networking Research Team until 1999. Since 1999, he has been a Professor with the Department of Computer Science and Engineering, Kyung Hee University. His research interests include future Internet, intelligent edge computing, network management, and network security. Dr. Hong is a member of ACM, IEICE, IPSJ, KISE, KICS, KIPS, and OSIA. He was an Associate Editor of the IEEE TNSM and the IEEE JSAC.



Nguyen H. Tran (S'10-M'11-SM'18) received BS and PhD degrees (with best PhD thesis award), from HCMC University of Technology and Kyung Hee University, in electrical and computer engineering, in 2005 and 2011, respectively. Dr Tran is an Associate Professor at the School of Computer Science, The University of Sydney. He was an Assistant Professor with Department of Computer Science and Engineering, Kyung Hee University, from 2012 to 2017. His research group has special interests in Distributed computing, optimization, and machine Learning (DUAL group). He received several best paper awards, including IEEE ICC 2016 and ACM MSWiM 2019. He receives the Korea NRF Funding for Basic Science and Research 2016-2023, ARC Discovery Project 2020-2023, and SOAR award 2022-2023. He has been on the Editorial board of several journals such as IEEE Transactions on Green Communications and Networking (2016-2020), IEEE Journal of Selected Areas in Communications 2020, and IEEE Transactions on Machine Learning in Communications Networking (2022-).